

Report 2259-1

AD 641 6



DEPARTMENT OF THE NAVY

WIND TUNNEL INVESTIGATION OF AN ASPECT RATIO 10 TANDEM WING AIRCRAFT CONFIGURATION IN GROUND EFFECT  
PART I - LONGITUDINAL CHARACTERISTICS

by

Charles W. Harry and Lynn A. Trobaugh

The distribution of this document is unlimited.

HYDROMECHANICS

AERODYNAMICS

STRUCTURAL MECHANICS

APPLIED MATHEMATICS

ACOUSTICS AND VIBRATION

CLEARINGHOUSE FOR FEDERAL SCIENTIFIC AND TECHNICAL INFORMATION		
Hardcopy	Microfiche	
\$3.00	\$ .75	7/1/66
/ ARCHIVE COPY		

REC'D  
NOV 4 1966

AERODYNAMICS LABORATORY  
RESEARCH AND DEVELOPMENT REPORT

July 1966

Report 2259-1

WIND TUNNEL INVESTIGATION OF AN ASPECT RATIO 10 TANDEM  
WING AIRCRAFT CONFIGURATION IN GROUND EFFECT  
PART I - LONGITUDINAL CHARACTERISTICS

by

Charles W. Harry and Lynn A. Trobaugh

Bureau of Naval Weapons  
Problem Assignment 1-34-52

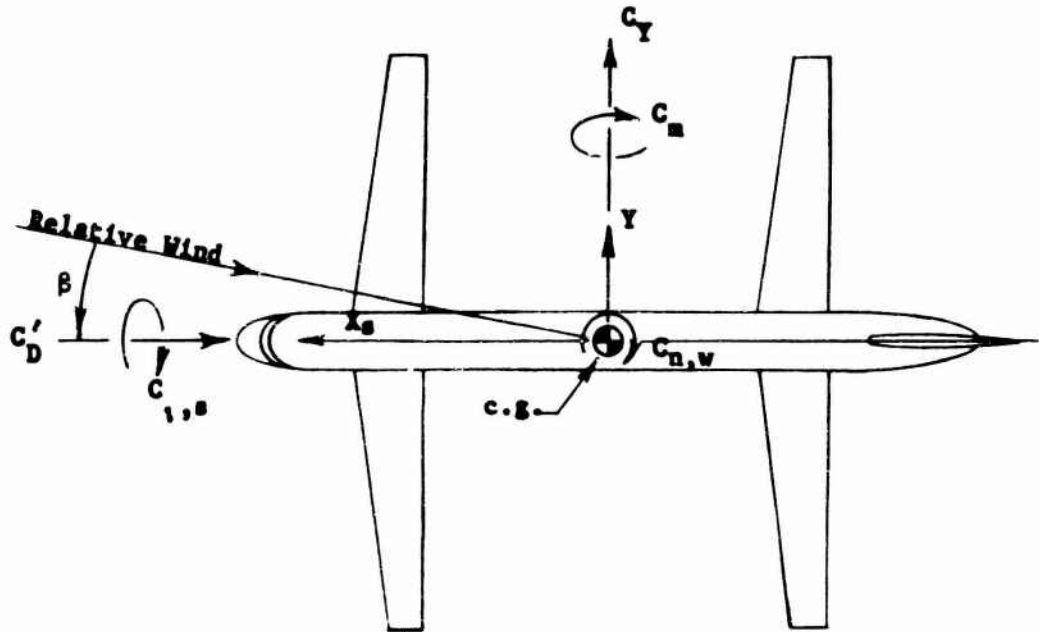
The distribution of this document is unlimited.

July 1966

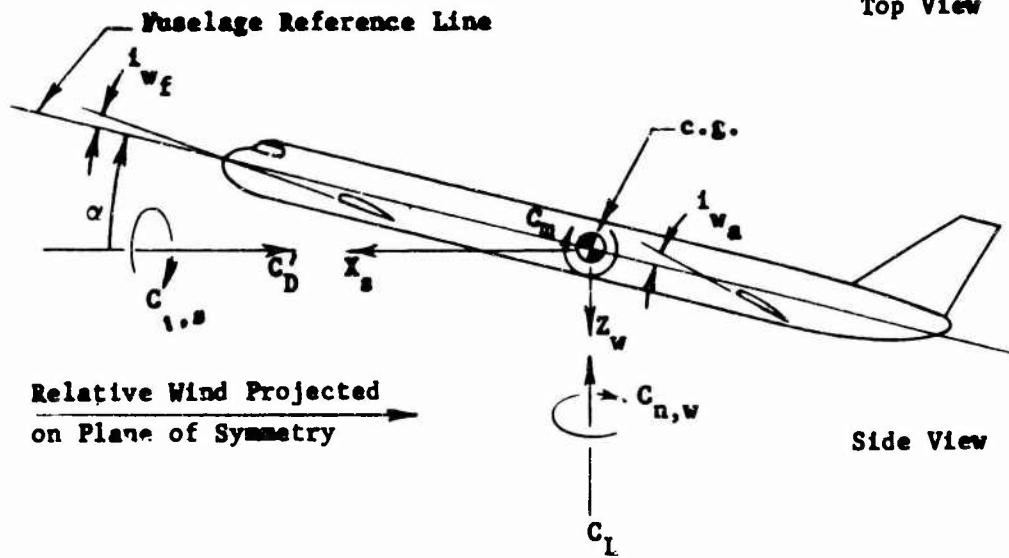
Report 2259-1  
Aero Report 1111-1

### NOTATION

Positive directions of axes, forces, moments, and angular displacements are shown by arrows.



Top View



Side View

Axis	Force in pounds	Force Coefficient	Moment in pound-feet	Moment Coefficient
$X_s$	$F'_D$	$C'_D = F'_D / qS$	$M_{X_s}$	$C_{l,s} = M_{X_s} / qSb$
$Y$	$F_Y$	$C_Y = F_Y / qS$	$M_Y$	$C_m = M_Y / qS\bar{c}$
$Z_w$	$F_L$	$C_L = F_L / qS$	$M_{Z_w}$	$C_{n,w} = M_{Z_w} / qSb$

### SYMBOLS

A	wing geometric aspect ratio ( $b^2/S$ )
$A_e$	wing effective aspect ratio $\left( \frac{1}{\pi} \frac{dC_L^2}{dC_D} \right)$
b	wing span in feet
$\bar{c}$	mean geometric chord of wing in feet
$C'_D$	drag coefficient ( $D'/qS$ )
c.g.	center of gravity
$C_L$	lift coefficient ( $L/qS$ )
$C_m$	pitching moment coefficient $\left( \frac{\text{pitching moment}}{qS\bar{c}} \right)$
$D'$	aerodynamic drag in pounds
h	height in feet (measured vertically from the ground board to a point directly below the c.g. in the plane defined by the trailing edges of both wings)
$i_w$	wing incidence angle in degrees (wing reference line taken as bottom of Clark Y section)
$\Delta i_w$	difference in incidence angle on the forward and aft wing $\left( \Delta i_w = i_{w_a} - i_{w_f} \right)$
L	lift in pounds
r	distance in feet aft of the forward c.g. location to any other desired c.g. location
S	total wing area (two wings) in square feet
W	gross weight in pounds
$\alpha$	angle of attack in degrees (angle between fuselage reference line and relative-wind vector)

### Subscripts

a	aft c.g. location or aft wing
f	forward c.g. location or forward wing
m	mid c.g. location
max	maximum

## TABLE OF CONTENTS

	Page
NOTATION	ii
SYMBOLS	iii
SUMMARY	1
INTRODUCTION	1
MODEL AND EQUIPMENT	2
TESTS	3
RESULTS	4
DISCUSSION	7
LIFT-DRAG CHARACTERISTICS	7
LONGITUDINAL STABILITY	9
LONGITUDINAL TRIM	11
CONCLUSIONS	11
REFERENCES	13

### LIST OF TABLES

Table 1 - Physical Characteristics of a 1/40-Scale Model TWIG	14
---	----

### LIST OF ILLUSTRATIONS

Figure 1 - Principal Dimensions of a 1/40-Scale Model Tandem Wing In Ground Effect	15
Figure 2 - Side View of Tunnel Installation Showing Inverted Model and Telescoping Strut	16
Figure 3 - Longitudinal Aerodynamic Characteristics of the TWIG Model With $i_{w_f} = i_{w_a} = 0^\circ$	17-22
Figure 4 - Longitudinal Aerodynamic Characteristics of the TWIG Model With $i_{w_f} = i_{w_a} = 2^\circ$	23-28
Figure 5 - Longitudinal Aerodynamic Characteristics of the TWIG Model With $i_{w_f} = i_{w_a} = 4^\circ$	29-34
Figure 6 - Longitudinal Aerodynamic Characteristics of the TWIG Model With $i_{w_f} = i_{w_a} = 8^\circ$	35-38
Figure 7 - Performance Parameters of Trimmed TWIG Model at Mid c.g. $\alpha = 0^\circ$	39
Figure 8 - Forward Wing Effectiveness of the TWIG Model With a Mid c.g. Location and $i_{w_a} = \alpha = 0^\circ$	40

TABLE OF CONTENTS (Concluded)

	Page
Figure 9 - Aft Wing Effectiveness of the TWIG Model With a Mid c.g. Location and $i_{w_f} = \alpha = 0^\circ$	41
Figure 10 - Effect of $i_{w_a}$ on the TWIG Model Lift Performance With $\alpha = 0^\circ$	42-44
Figure 11 - Required $i_{w_a}$ for Trim of the TWIG Model In Ground Effect	45-49
Figure 12 - Longitudinal Aerodynamic Characteristics of the TWIG Model Out of Ground Effect ( $h/b = \infty$ )	50-51
Figure 13 - Required $i_{w_a}$ for Trim of the TWIG Model Out of Ground Effect	52-57
Figure 14 - Difference in Wing Incidence Angles Required for Trim of the TWIG Model Out of Ground Effect	58
Figure 15 - Longitudinal Aerodynamic Characteristics of the TWIG Model Out of Ground Effect With the Aft Wing Removed	59-60
Figure 16 - Summary of TWIG Model Trim Data In and Out of Ground Effect. $\alpha = 0^\circ$	61

BLANK

## SUMMARY

Subsonic wind-tunnel test results of a tandem-wing aircraft model investigated in and out of ground effect are given. Test variables included model height above a ground board, model angle of attack, forward and aft wing incidence angles, and center-of-gravity location.

Ground effect, by increasing the lift of the wings and reducing their drag, provided a substantial increase in the lift/drag ratio of the model. For example, the lift/drag ratio of the model was increased by a factor of 2 as a result of ground proximity when the model was closest to the ground board.

Static longitudinal stability of the model is very sensitive to center-of-gravity location. Of the three center-of-gravity locations tested, only the forward and mid locations provided longitudinal stability. The mid center-of-gravity location is preferred because, at this position, the model could be trimmed with less difference in the fore and aft wing incidence angles. This resulted in slightly improved lift/drag ratio.

## INTRODUCTION

The aerodynamicist has long been familiar with the high lift/drag ratios possible for aircraft cruising continuously in close proximity to the earth's surface in order to exploit the suppression of induced drag by ground effect. As presently envisioned, interface vehicles utilizing this effect appear practical only for large craft. Because of the dearth of experimental aerodynamic data on the ground-effect phenomenon, it was felt that a configuration study would be incomplete without some answers to questions which include stability and control.

Earlier DTMB tests of a wing-in-ground-effect (WIG), presented in Reference 1, indicated very good altitude or heave stability but poor pitch stability, making longitudinal control difficult. This led to the consideration of an equal-span, tandem-wing configuration as a solution to the WIG's longitudinal control problem. This model, referred to as a TWIG (tandem wing in ground effect), was tested in the DTMB 8-by 10-Foot Subsonic Wind Tunnel in the presence of a ground board to simulate ground effect. A wing with an aspect ratio of 10 was chosen



for the model because it was felt that this aspect ratio was optimum as far as structural feasibility and high lift/drag ratios were concerned. The model was also tested out of ground effect. Longitudinal aerodynamic characteristics of the TWIG model are presented in this report. A lateral stability study was also made and the results will be made available in a forthcoming report (Reference 2).

#### MODEL AND EQUIPMENT

A 1/40-scale model of a hypothetical TWIG configuration was designed and constructed at DTMB. The geometry and principal dimensions of the model are presented in Figure 1. A listing of the physical characteristics of the model is given in Table 1. The model represents a craft having a wing span of 200 feet.

The fuselage of the model consists of an aluminum box veneered with a 1/2-inch thickness of mahogany on the sides, top, and bottom. Carved mahogany nose and tail blocks were attached to the aluminum box to create a streamlined fuselage. A hinged mounting pad in the fuselage controlled by a jackscrew provided a method of varying the angle of attack of the model.

A Clark Y airfoil section was used for each of the two wings. Both wings were constructed of fiberglass with embedded steel spars to improve wing stiffness. The distance between the wings was chosen from the results of tandem wing tests in Reference 1. Each wing was mounted on a bracket which was constructed so that the incidence angle could be varied. The brackets were hinged so that rotation of the wing occurred about its trailing edge. Each mounting bracket had its own adjusting jackscrew so that the incidence angle of either wing could be varied independently. The wings and the vertical tail had no control surfaces.

A special, telescoping mounting strut was constructed for the test. When the strut with the model attached was installed in the tunnel, the model could be translated vertically through a distance of nine inches. The strut was also capable of being yawed through an angle of  $\pm 25^\circ$ . Details of the strut are shown in Figure 2.

For the ground-effect tests, a metal ground board was installed in the tunnel so that when the strut was fully extended, the model was closest to the ground board. Conversely, when the strut was retracted, the model was at a distance of about nine inches from the ground board. The model was mounted in an inverted position on the strut for the in-ground-effect tests and upright for the out-of-ground-effect tests.

#### TESTS

All tests were conducted in the DTMB 8- by 10-Foot Subsonic Wind Tunnel at a dynamic pressure of 50 pounds per square foot. For the TWIG model, this corresponds to a Reynolds number of approximately 654,000.

In-ground-effect tests of the TWIG model were conducted at heights of 1.8 to 9.0 inches, through an angle-of-attack range from  $-2^\circ$  to  $+6^\circ$ . Longitudinal force and moment data were recorded and reduced by digital computer. The large number of test variables involved prevented a complete investigation of all resultant matrix quantities. However, sufficient tests were conducted and data recorded to determine trends of interest.

The model support apparatus, Figure 2, caused a change in the height parameter  $h/b$  with the variation of fuselage angle of attack. The reference height  $h$  was determined at  $\alpha = 0^\circ$  as the vertical distance from the ground board to the plane of the trailing edges of the wings. Test data were first reduced to the forward center-of-gravity location. The following transfer equations were then employed in the computer program to calculate the data to the mid and aft center-of-gravity locations.

$$\frac{h_m}{b} = \frac{h_f - r_m \sin \alpha}{b}$$

$$\frac{h_a}{b} = \frac{h_f - r_a \sin \alpha}{b}$$

$$C_{m_m} = C_{m_f} + \frac{r_m}{\bar{c}} (C_L \cos \alpha + C_D' \sin \alpha)$$

$$C_{m_a} = C_{m_f} + \frac{r_a}{\bar{c}} (C_L \cos \alpha + C_D' \sin \alpha)$$

For the TWIG model,  $r_m$  and  $r_a$  have the values of 0.25 and 0.50 feet, respectively. Data for other center-of-gravity locations may be computed, if desired, merely by substituting the proper value of  $r$  into the above equations.

The in-ground-effect data were obtained by using a ground board to simulate the earth's surface. A pressure survey was conducted over the ground board to determine the boundary layer thickness in the vicinity of the model. The boundary layer thickness in this region was only about 0.75 inch, which is well below the minimum wing-to-ground-board clearance of 1.8 inches.

### RESULTS

The nondimensional parameter, height/span ( $h/b$ ), has proven useful in the study of ground-effect phenomena. Therefore, the data were prepared for presentation as follows: (a) longitudinal aerodynamic coefficients were plotted against height/span for each center-of-gravity position (forward, mid, and aft), (b) values of the coefficients were read from these plots for several values of height/span ratio (0.03 to 0.15) for each center-of-gravity position, and (c) plots were made using these values of the aerodynamic coefficients.

Longitudinal aerodynamic characteristics of the TWIG model with various equal wing incidence angles ( $i_{w_f} = i_{w_a}$ ) are presented in Figures 3 through 6. Curves for all three center-of-gravity locations are presented for each value of ( $i_{w_f} = i_{w_a}$ ) tested (namely,  $0^\circ$ ,  $2^\circ$ ,  $4^\circ$ , and  $8^\circ$ ), except at the highest incidence angle (Figure 6), where the forward center-of-gravity location is omitted.

The TWIG performance parameters:  $(L/D)_{\max}$ ,  $C_L$  at  $(L/D)_{\max}$ , and  $A_e/A$  are given in Figure 7. The experimental curves were obtained from the fitted values of the data similar to the data shown in Figures 3 through 6. Several curves of  $A_e/A$  are shown. The predicted curve was obtained by correcting the TWIG drag polar for out-of-ground-effect flight to drag polars for in-ground-effect flight, at a number of  $h/b$ 's, using correction factors from Reference 3. The values of  $A_e$  for the predicted and the experimental curves were computed from the equation:

$$A_e = \frac{1}{\pi} \left( \frac{dC_L^2}{dC_D'} \right)$$

where the slope  $\frac{dC_L^2}{dC_D'}$  was determined graphically from plots of  $C_L^2$  versus  $C_D'$  (Reference 4). The theoretical curve of  $A_e/A$  for this figure was obtained from Reference 3.

Figures 8 and 9 show the effectiveness of the forward and aft wings, respectively, as longitudinal control and/or trim devices. In Figure 8, the forward wing acts as a canard with  $i_{w_a}$  and  $\alpha$  held equal to zero. Conversely, in Figure 9, the aft wing is used as an elevator with  $i_{w_f}$  and  $\alpha$  held equal to zero. Both of these figures are for the mid center of gravity only.

Shown in Figure 10 is the effect of  $i_{w_a}$  on the lift performance of the TWIG. These curves are applicable to all three center-of-gravity locations, since  $\alpha$  was held constant at zero for this series of tests. In each part of the figure,  $i_{w_f}$  was set at some new value and held there for the range of  $i_{w_a}$  tested.

Trim data for the TWIG model in-ground-effect is given in Figure 11. Because of insufficient data, it was necessary to extrapolate the existing data slightly to obtain trim points. Higher  $\alpha$ 's restricted the lowest  $h/b$  to values greater than 0.063 because of ground clearance. For this reason, in part (a) of Figure 11, the maximum  $\alpha$  is  $2^\circ$ . Values of  $h/b$  lower than 0.05 are not given, since it was physically impossible to operate the model over a sufficiently large range of  $\alpha$ 's.

Figures 12 through 15 present data on the TWIG model out of ground effect. Figure 12 shows the longitudinal aerodynamic characteristics for  $i_{w_f} = 0^\circ$ , and  $i_{w_a}$  restricted to small angles. Pitching moment coefficients and lift coefficient curves for all three center-of-gravity locations are given in the same figure. The aft wing incidence angle was varied slightly to show the power of  $i_{w_a}$  in changing  $C_m$ .

Figure 13 is a presentation of the model data out of ground effect. This figure contains data for trimmed flight ( $C_m = 0^\circ$ , only). The symbols in the figure show what value of  $i_{w_a}$  is required for a given  $i_{w_f}$  to trim the model. A curve for each of the three center-of-gravity locations is presented. Should values of  $i_{w_f}$  other than those represented by the symbols be desired, they can be obtained by interpolating linearly between the symbols on a given center-of-gravity curve. In addition, values of  $i_{w_f}$  required for trim at center-of-gravity locations lying between those represented by the curves may be obtained by interpolating linearly between the center-of-gravity curves on a given  $i_{w_f}$  curve. Also given in Figure 13 are curves of the L/D ratios of the trimmed model flying out of ground effect.

Figure 14 was derived from the data of Figure 13. It shows how different wing incidence angles on the forward and aft wings affect the lift performance. In Figure 14,  $\Delta i_w$  was computed from the equation

$$\Delta i_w = i_{w_a} - i_{w_f}$$

Thus, positive values of  $\Delta i_w$  indicate that  $i_{w_a} > i_{w_f}$  and, conversely, negative values of  $\Delta i_w$  indicate  $i_{w_a} < i_{w_f}$ .

Longitudinal aerodynamic characteristics of the TWIG model flying out of ground effect with the aft wing removed are presented in Figure 15. This figure is comparable to the tandem wing model configuration data of Figure 12. In Figure 15, data are presented to give some indication of the interference effects of the forward wing upon the aft wing.

The trim data of the TWIG model, both in and out of ground effect, are given in Figure 16. This figure is presented to summarize the in- and out-of-ground-effect data. In-ground-effect data were obtained from the linear interpolation of plots similar to Figures 3 through 6 to obtain values of the coefficients at trim conditions. Out-of-ground-effect data were obtained from plots presented earlier in this report.

Only data for the mid center-of-gravity location are given and only for  $\alpha = 0^\circ$ .

Unless otherwise noted, the data presented in the above-mentioned figures are for the in-ground-effect case. Out-of-ground-effect flight would be required only for high sea states and for clearing large obstacles such as those that might be encountered in arriving at or departing from an inland airport.

## DISCUSSION

The primary purpose of these tests was to determine the aerodynamic characteristics of a tandem wing configuration operating in and out of ground effect. The discussion is subdivided into these sections: Lift/ Drag Characteristics, Longitudinal Stability, and Longitudinal Trim.

### LIFT-DRAG CHARACTERISTICS

Figure 7 shows a comparison of the TWIG model wind-tunnel test results and the predicted in-ground-effect performance with the theory of Reference 3. As can be seen from the figure, the experimental and predicted results are in good agreement with theory, even though several simplifying assumptions are made by theory. It was found that the tandem-wing configuration behaved as though its aspect ratio ( $A = \frac{b^2}{S}$ ) were 5 instead of the individual wing aspect ratio of 10. The experimental and predicted curves of  $A_e/A$  were both computed using  $A = 5$ . The theoretical curve is independent of aspect ratio. If  $A = 10$  had been used in computing the experimental and predicted curves, values of  $A_e/A$  for both curves would be only half of those which were obtained using  $A = 5$ . The theoretical curve would not be changed.

Values of  $C_L$  at  $(L/D)_{\max}$  for the TWIG model in ground effect are higher than desired. For example, at a practical  $h/b$  of 0.10 at the mid center-of-gravity location, the required value of  $C_L$  is about 0.55 (see Figures 11d and 16). Figure 7 shows that, at the mid center-of-gravity location,  $C_L$  for  $(L/D)_{\max}$  is high for all values of  $h_m/b$ , the lowest  $C_L$  value being 0.53 for  $h_m/b = 0.15$  and the highest  $C_L$  value being 0.70 for  $h_m/b = 0.03$ . Furthermore, as can be seen in Figure 11, if  $i_{wf}$  is set at a value greater than zero, the  $C_L$  for  $(L/D)_{\max}$  has even larger values than the curve of Figure 7. Further examination of

Figure 16 reveals that, as higher  $L/D$  ratios are sought, hence requiring lower values of  $h/b$ , the  $C_L$  value required for trimmed cruise flight at  $(L/D)_{\max}$  increases. As can be seen from Figure 16, high values of  $C_L$  for  $(L/D)_{\max}$  also occur with the model flying out of ground effect. Thus, it is not possible to conclude that these high  $C_L$  values are a characteristic of in-ground-effect flight. It is possible that lower values of  $C_L$  for  $(L/D)_{\max}$  may be obtained by using a thinner airfoil section.

High values of  $C_L$  present several problems. If high cruise velocities are desired (i.e., about 200 knots), wing loadings would be undesirably higher than currently accepted values. These high wing loadings would require that the take-off and landing speeds be a very high percentage of the cruise velocity unless the value of  $C_L$  at take-off and landing can be significantly increased with high-lift devices—an unlikely event, considering the ineffectiveness of flaps in ground effect. On the other hand, currently acceptable wing loadings can be obtained only by sacrificing high cruise velocity.

The effects of wing incidence angles on lift performance are shown in Figures 3 through 6 for the model flying in ground effect. A comparison of these figures reveals that, for a given center-of-gravity location, as  $i_{w_f}$  and  $i_{w_a}$  are increased equally, the slopes of the  $C_L$  versus  $C_D'$  curves decrease slightly. This would indicate that the aircraft should be flown at the lowest incidence angles possible so that the lowest possible value of  $C_L$  for  $(L/D)_{\max}$  may be used.

For trimmed cruising flight in ground effect, the value of  $(L/D)_{\max}$  is increased over the value of  $(L/D)_{\max}$  out of ground effect by a factor of about 2. For example, in Figure 16, the maximum value of  $L/D$  out of ground effect is about 16.5. In ground effect, for  $h_m/b = 0.03$ , the maximum value of  $L/D$  is 33.

The effects of center-of-gravity location on lift/drag characteristics with the model trimmed are shown in Figure 11. Effects of mutual

wing interference are evident in the reflex in the L/D curves of the figure. Interference effects become more pronounced at lower values of  $i_{w_f}$  and at the aft center-of-gravity location. Figure 11 also shows that higher L/D values are available at the aft center-of-gravity location. For a given h/b, values of L/D at a given  $C_L$  may be as much as 10 percent higher at the aft center-of-gravity location than at the forward center-of-gravity location.

#### LONGITUDINAL STABILITY

Conventional aircraft obtain longitudinal stability from the fact that the pitching moment contribution of the horizontal stabilizer (with its change of lift on a long moment arm) exceeds the change in pitching moment of the wing when the aircraft is disturbed from equilibrium. Out of ground effect, the TWIG obtains stability in the same manner. Hence, as with a conventional aircraft, as the center-of-gravity position of the TWIG is moved aft, the longitudinal stability of the model decreased (the moment arm to the aft lifting surface was reduced).

It was hoped that the stability of the tandem wing configuration for in-ground-effect flight would be augmented by the individual wing contribution from a change in lift as a result of the change in each wing's operational height for a pitch displacement of the model. That is, if the model were pitched nose up, the lift on the front wing would decrease as a result of the increase in its effective operational height. Simultaneously, there would be an increase in the lift of the aft wing as its height decreased. Thus, a restoring pitching moment is formed which, it was hoped, along with craft basic stability would result in a very stable configuration.

However, simultaneously the moment in ground effect is reduced because, even with the TWIG pitched nose up, the forward wing is still in proximity to the ground and, as a result, its downwash is restricted. This reduction in downwash results in a reduction of the aft wing contribution to longitudinal stability, since its change in angle of attack is reduced. Nevertheless, the TWIG configuration is substantially more stable in ground effect than out of ground effect.



Pitching moment data were obtained for three different center-of-gravity locations. The locations on the model are shown in Figure 1. The aft center-of-gravity location is stable only over a small operational range, but this range does occur at  $(L/D)_{\max}$ . The forward and mid center-of-gravity locations are stable, with the mid center-of-gravity location possessing some regions of instability. However, only the mid center-of-gravity location could be trimmed with a small  $\Delta i_w$ , which led to superior L/D ratios.

One of the more desirable stability characteristics of any type of aircraft is that the pitching moment coefficient should vary linearly with  $C_L$  in the flight spectrum. Of the three center-of-gravity locations tested for the TWIG model, the forward center-of-gravity location most nearly results in linear  $C_m$  to  $C_L$  variation (i.e., a constant stability derivative,  $\frac{dC_m}{dC_L}$ ); however, even it departs significantly from being completely linear. Figures 3 through 6 show a hump in the pitching moment coefficient curves above an h/b of 0.07, which is present at all three center-of-gravity locations. As  $i_{w_f}$  and  $i_{w_a}$  are increased equally, the hump occurs at higher  $C_L$  values and tends to flatten out at higher values of  $i_{w_f} = i_{w_a}$ . The hump in the curves appears to be caused by the mutual interference effects of tandem wings.

Figure 15 shows the pitching moment curves of the TWIG model with the aft wing removed. As can be seen from this figure, the curves are linear. However, when the aft wing is placed on the model and flown in ground effect, the pitching moment curves are no longer linear and the hump appears in the curves. Pitching moment curves are not linear for the out-of-ground-effect case either, as can be seen from Figure 12. The model is unstable out of ground effect for values of  $C_L$  below 0.6, the aft center of gravity being the most unstable. Above  $C_L$  values of 0.6, the model becomes stable. Such results suggest mutual wing interference as a cause of the non-linearity of the pitching moment curves.

Insufficient data were taken to present curves of  $\frac{dC_m}{dC_L}$  for the model. However, the curves of Figures 3 through 5 may be used in

conjunction with the trim curves of Figure 11 to get an indication of stability with the model trimmed (small discrepancies in  $i_{w_f}$  should not change the slope of the  $C_m/C_L$  curve).

#### LONGITUDINAL TRIM

The extrapolated data of Figure 11 indicate that the model may be trimmed at any of the three center-of-gravity locations when flying in ground effect. However, for small values of  $i_{w_f}$ , trim at the forward center-of-gravity location may be accomplished only by using negative values of  $i_{w_a}$ . From a trim standpoint, the mid center-of-gravity location is preferred because it requires lower  $i_w$ 's and  $\Delta i_w$ 's to trim at operational values of L/D. The same applies to the out-of-ground-effect case, Figures 13 and 14. However, were it not for the instability of the aft center-of-gravity location, it would be preferred over the other two center-of-gravity locations, even though larger values of  $\Delta i_w$  are required for trim, because higher values of L/D are available.

Figures 8 and 9 show the effectiveness of the forward and aft wings as trim devices. In Figure 8, the forward wing is the trim device, and in Figure 9, the aft wing is used as the trim device. Both the forward and aft wings are equally effective as trim devices. It might be pointed out that the data of Figures 8 and 9 may be used to determine the amount of elevator power required for longitudinal control of the model. The wings can be assumed to be fixed at some incidence angle and the data in the figures correlated to the effects of a hinged control surface.

#### CONCLUSIONS

As a result of wind-tunnel tests on a TWIG model in and out of ground effect, it was concluded that:

1. Values of effective aspect ratio derived from the test results were in fairly good agreement with theory.
2. From the standpoint of longitudinal stability and trim, the mid center-of-gravity location is preferred over the other two locations. However, the mid center-of-gravity location is not completely satisfactory in that it becomes unstable at lower values of  $C_L$ . This trend of instability is especially true for the lower model heights investigated.

3. Largest values of  $L/D$  occurred at the aft center of gravity for a trimmed model.

4. Mutual wing interference appears to be a contributing factor in causing the non-linearity and regions of instability in the pitching-moment-coefficient curves, both in and out of ground effect.

5. With zero angle of attack and a trimmed model,  $(L/D)_{\max}$  was increased from 16.5 out of ground effect to 33 at an  $h_m/b$  of 0.3 in ground effect. This represents an increase by factor of 2.

6. Values of  $C_L$  for trimmed, cruise flight at  $(L/D)_{\max}$  in ground effect are undesirably high, starting at  $C_L = 0.53$  at  $h_m/b = 0.15$  and increasing to  $C_L = 0.70$  at  $h_m/b = 0.03$ . Such high  $C_L$  values for cruising flight are not compatible with practical wing loadings or practical take-off and landing speeds. Lower  $C_L$  values for  $(L/D)_{\max}$  might be achieved by using a thinner airfoil section.

7. Out of ground effect, the model is unstable at all three center-of-gravity locations for values of  $C_L$  below 0.6. As  $C_L$  is increased above 0.6, the model becomes stable except for the aft center-of-gravity location which, at best, becomes neutrally stable.

8. The model can be trimmed for any of the three center-of-gravity locations by varying the incidence angle of the aft wing. However, the model can be trimmed with small values of  $\Delta i_w$  only at the mid center-of-gravity location.

9. The drag and lift/drag results presented were not adjusted for Reynolds number effects or for effects of appendages, roughness, and other factors which might differ between the model and a full-scale aircraft. The results therefore indicate trends but do not directly indicate the absolute performance levels which might apply to full-scale aircraft.

Aerodynamics Laboratory  
David Taylor Model Basin  
Washington, D. C.  
July 1966

#### REFERENCES

1. Harry, Charles W. Wind Tunnel Investigation of Ground Effect on a Rectangular Wing of Several Moderate Aspect Ratios. Wash., Jul 1965. 65 p. incl. illus. (David Taylor Model Basin. Rpt. 1979. Aero Rpt. 1086)
2. Trobaugh, Lynn A. and Charles W. Harry. Wind Tunnel Investigation of an Aspect Ratio 10 Tandem Wing Aircraft Configuration in Ground Effect. Part II: Lateral Characteristics. (David Taylor Model Basin. Aero Rpt. 1111, Pt. 2) (In preparation)
3. Wiesselsberger, Carl. Wing Resistance Near the Ground (Über den Flügelwiderstand in der Nähe des Bodens). Wash., Apr 1922. 7 l. (National Advisory Committee for Aeronautics. Tech Memo 77) (Translation from Zeitschrift für Flugtechnik and Motorluftschiffahrt (Munich), v. 12, 31 May 1921, p. 145-147)
4. Dinnell, James H. Principles of Aerodynamics. 1st ed. N. Y., McGraw-Hill, 1949. p. 147

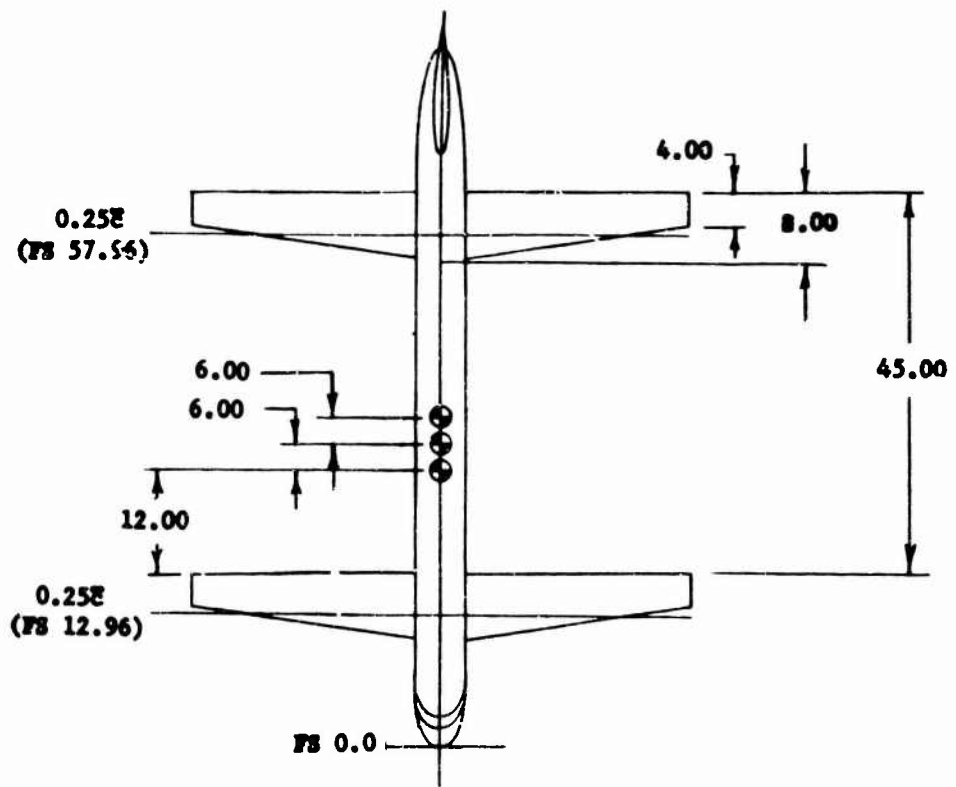
Table 1  
Physical Characteristics of a 1/40-Scale Model TWIG

Wing (Forward and aft are identical)

Airfoil section	Clark Y
Root chord in feet	0.667
Tip chord in feet	0.333
Taper ratio	0.5
Twist in degrees	0
Mean geometric chord in feet	0.50
Span in feet	5.0
Area in square feet	2.50
Aspect ratio	10
Sweep in degrees (1/4 chord)	1.91

Vertical Tail

Airfoil section	NACA 0012
Root chord in feet	1.000
Tip chord in feet	0.333
Taper ratio	0.333
Mean geometric chord in feet	0.721
Area in square feet	0.57
Sweep in degrees (1/4 chord)	45



All dimensions in inches.

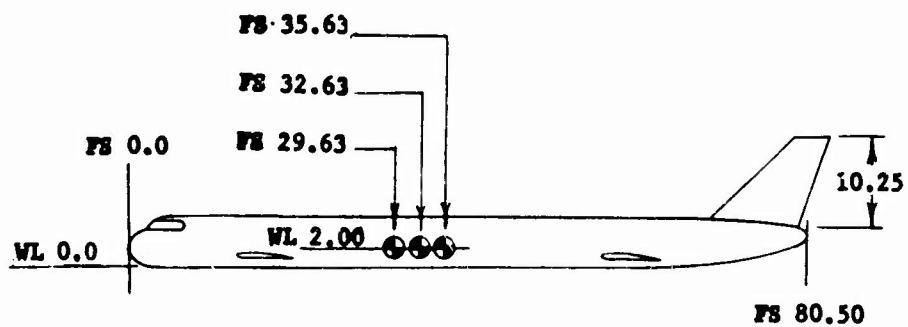
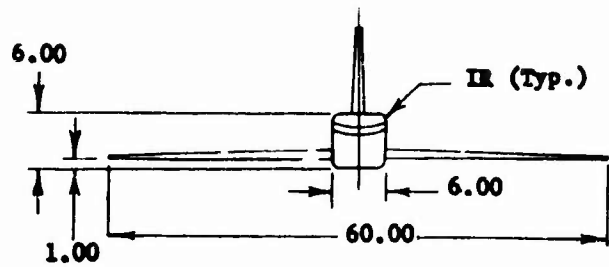


Figure 1 - Principal Dimensions of a 1/40-Scale Model  
Tandem Wing In Ground Effect

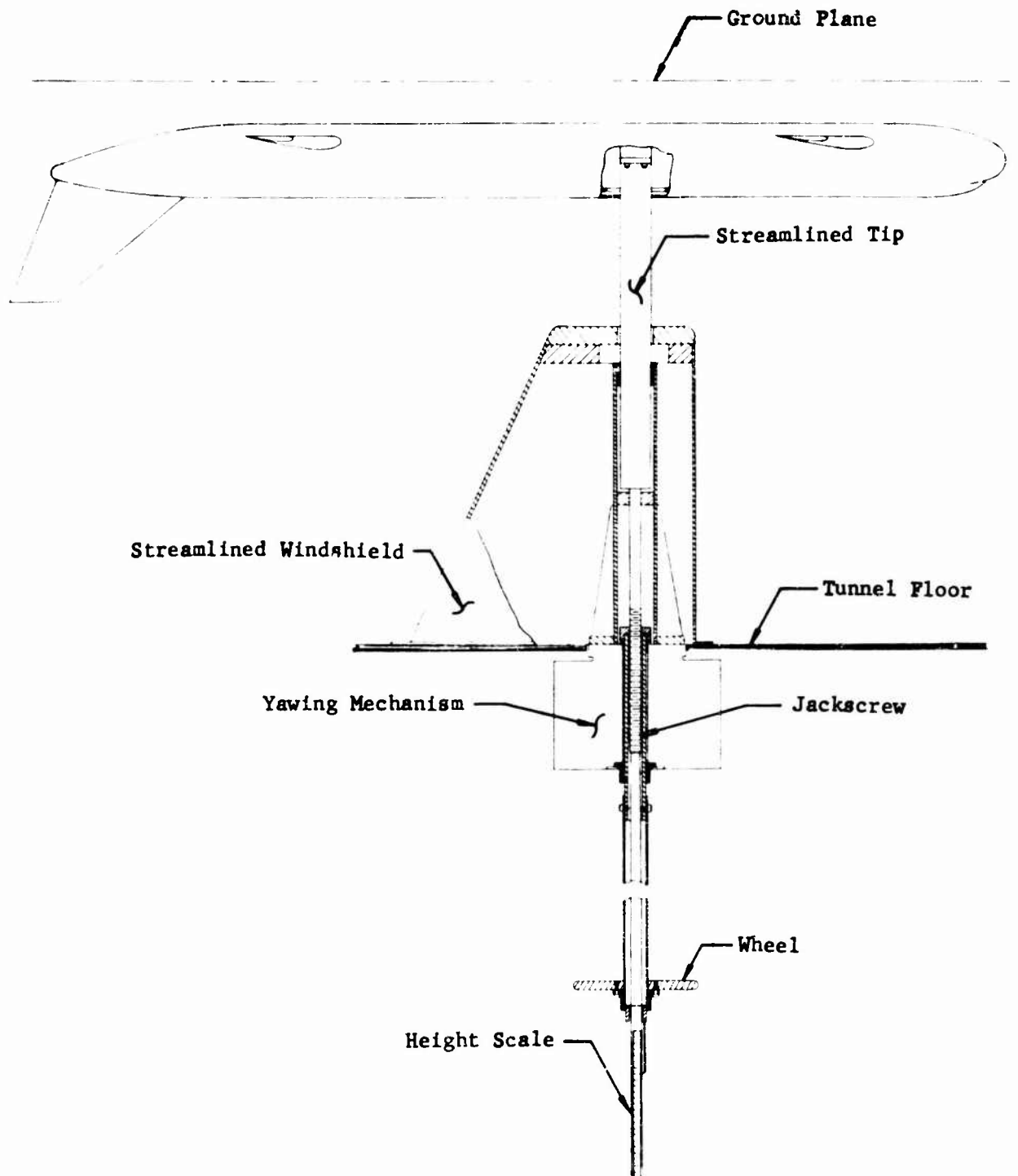


Figure 2 - Side View of Tunnel Installation Showing  
Inverted Model and Telescoping Strut

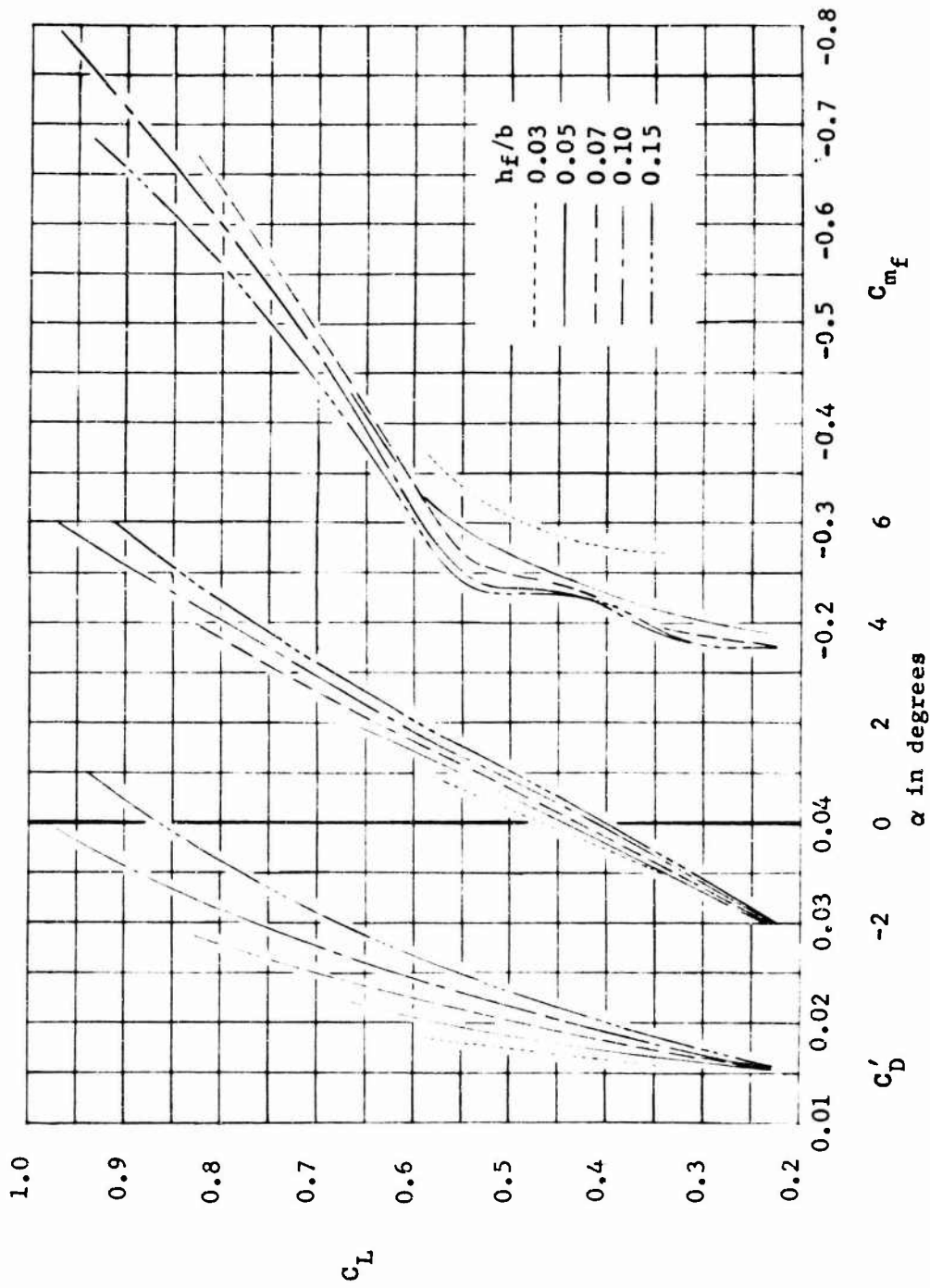


Figure 3 - Longitudinal Aerodynamic Characteristics of the

TWIG Model With  $i_{wf} = i_w = 0^\circ$

(a) Forward c.g.



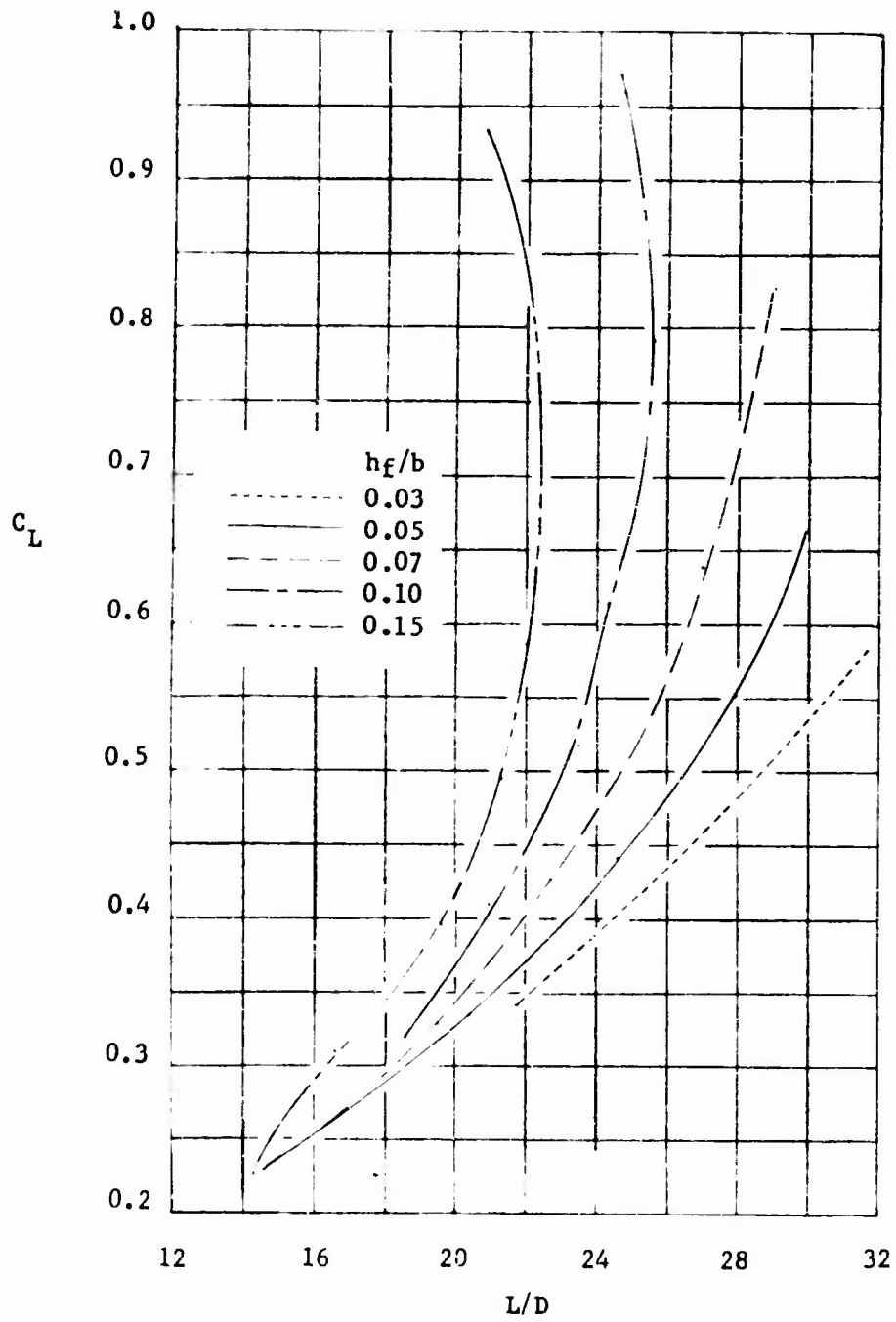


Figure 3 (Continued)  
(a) Concluded

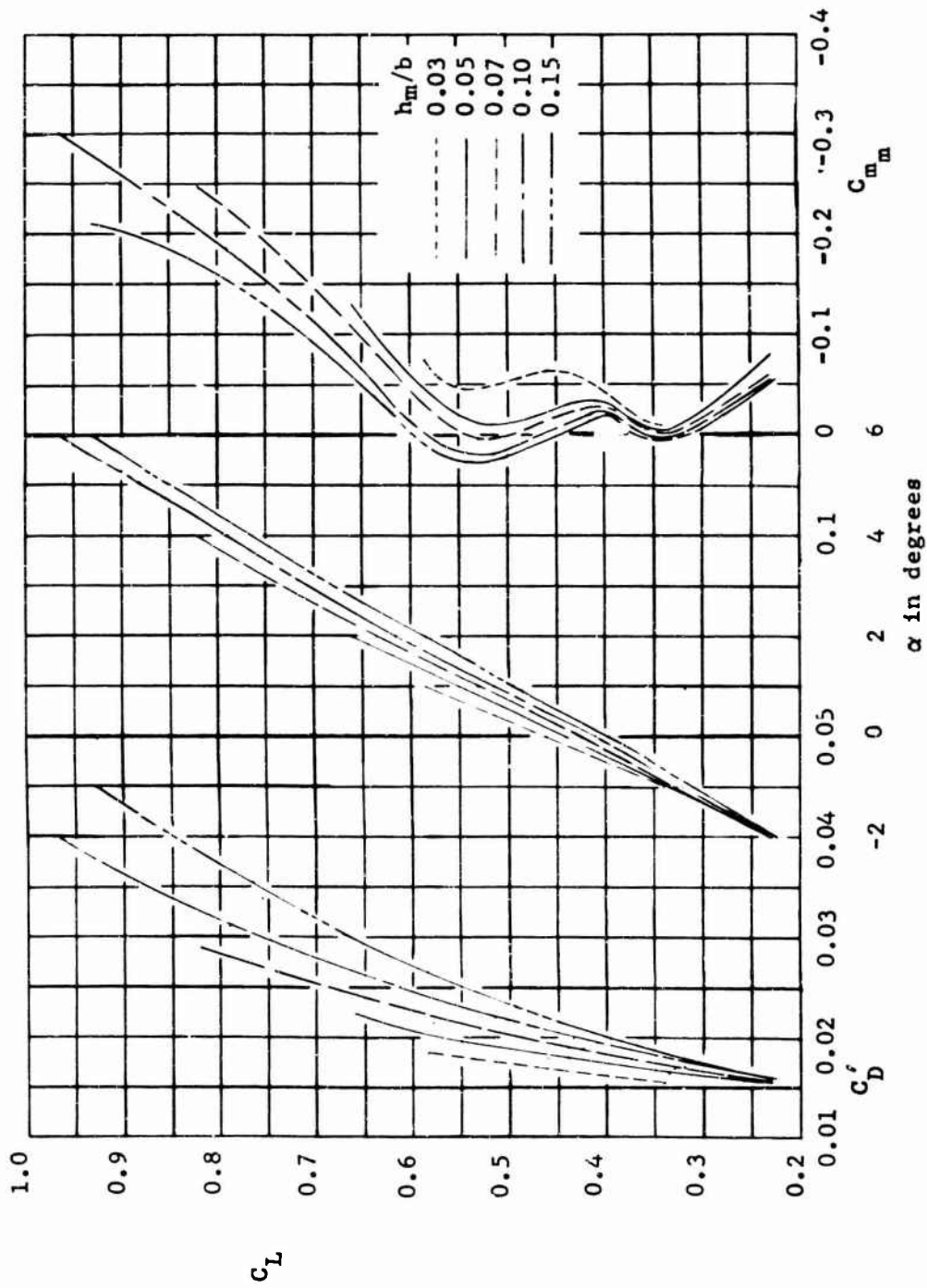


Figure 3 (Continued)

(b) Mid c.g.

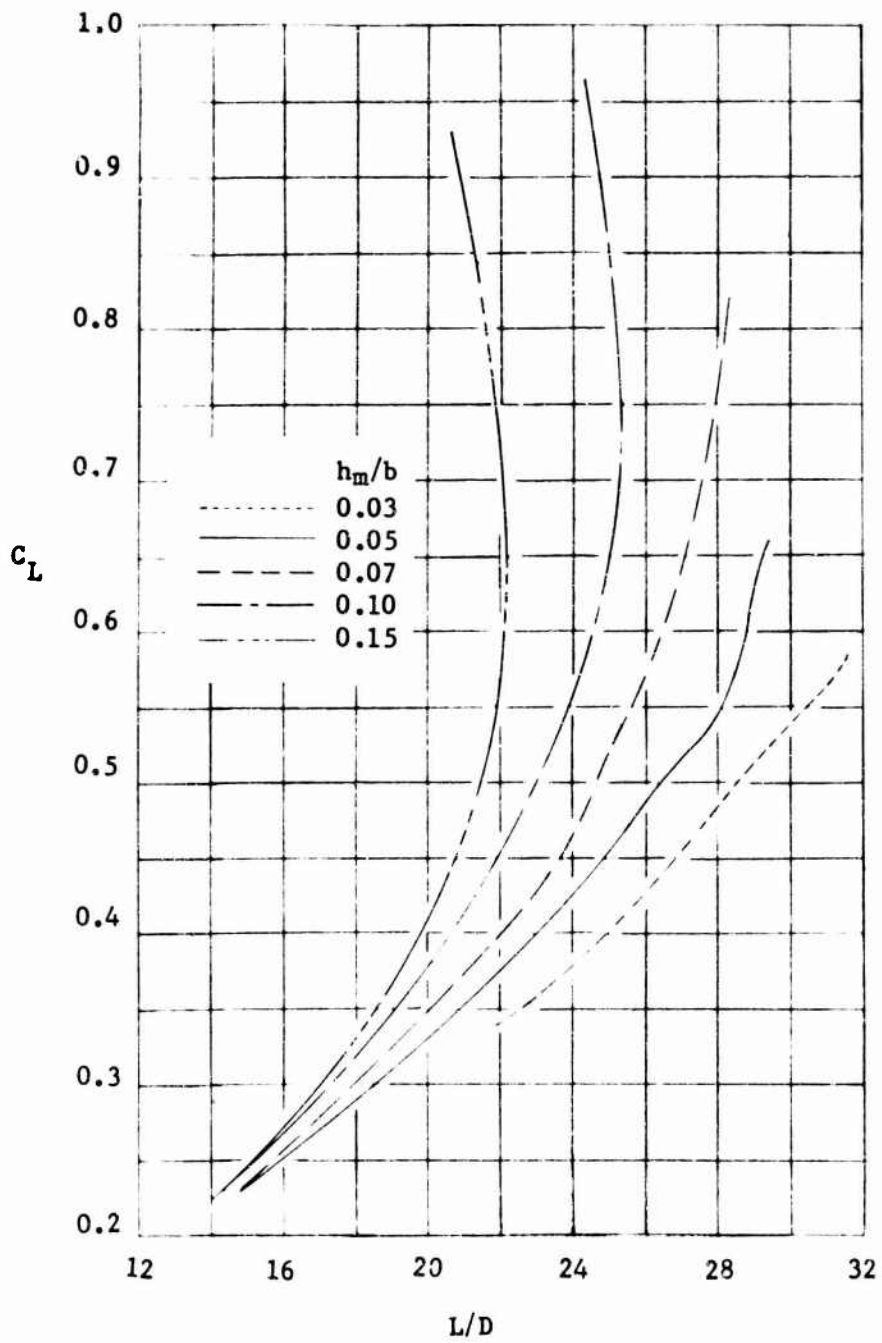


Figure 3 (Continued)

(b) Concluded

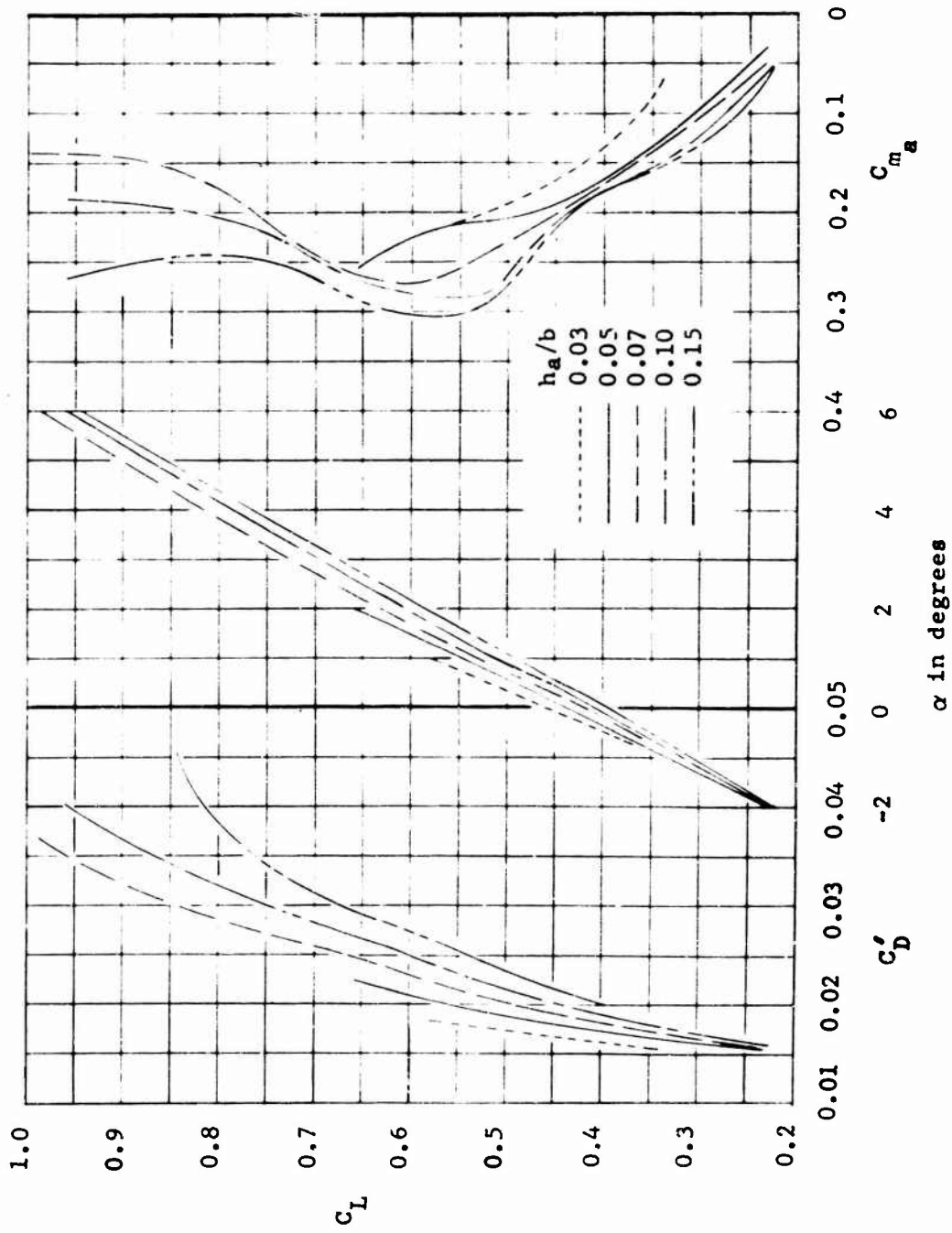


Figure 3 (Continued)  
 (c) Aft c.g.

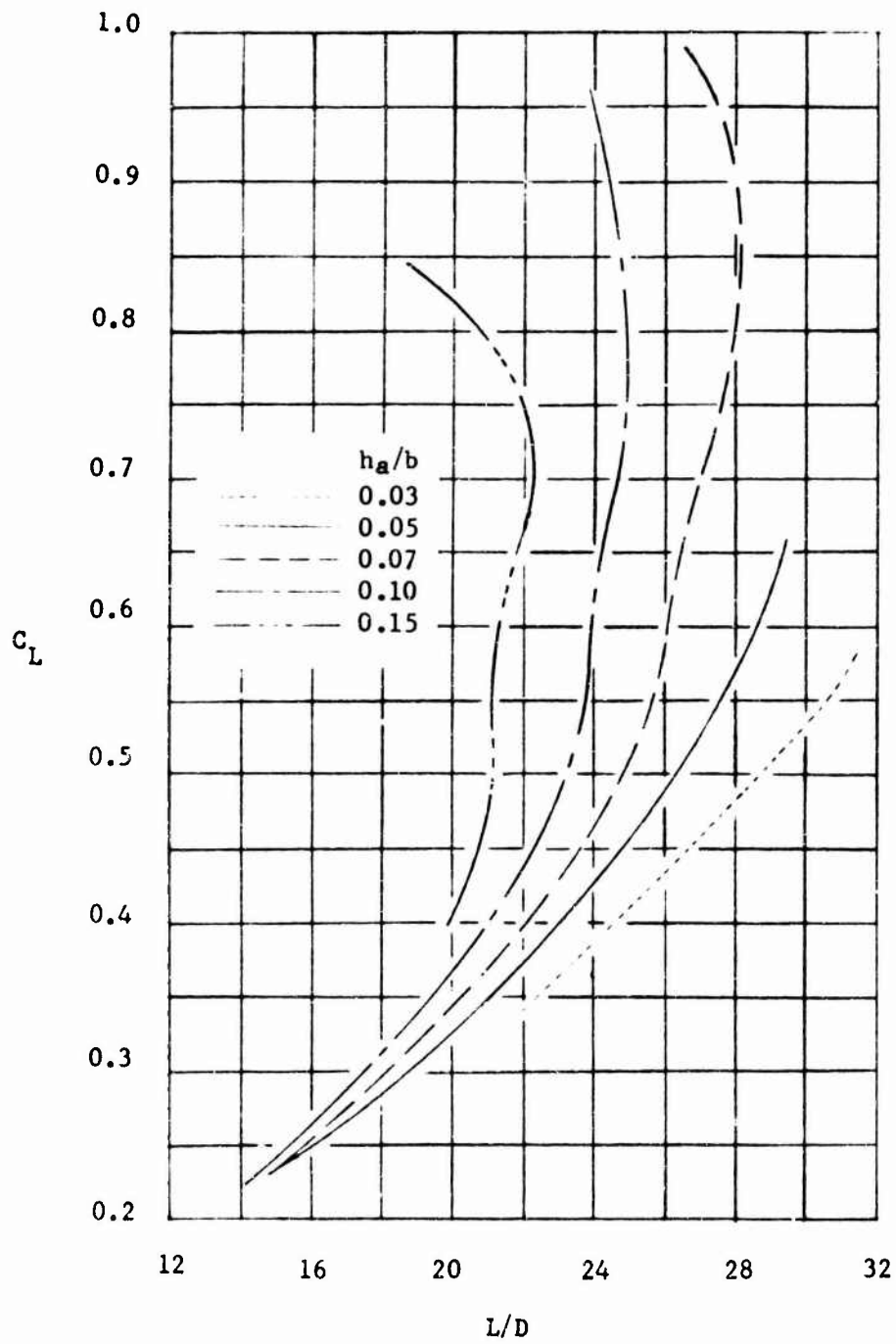


Figure 3 (Concluded)  
(c) Concluded

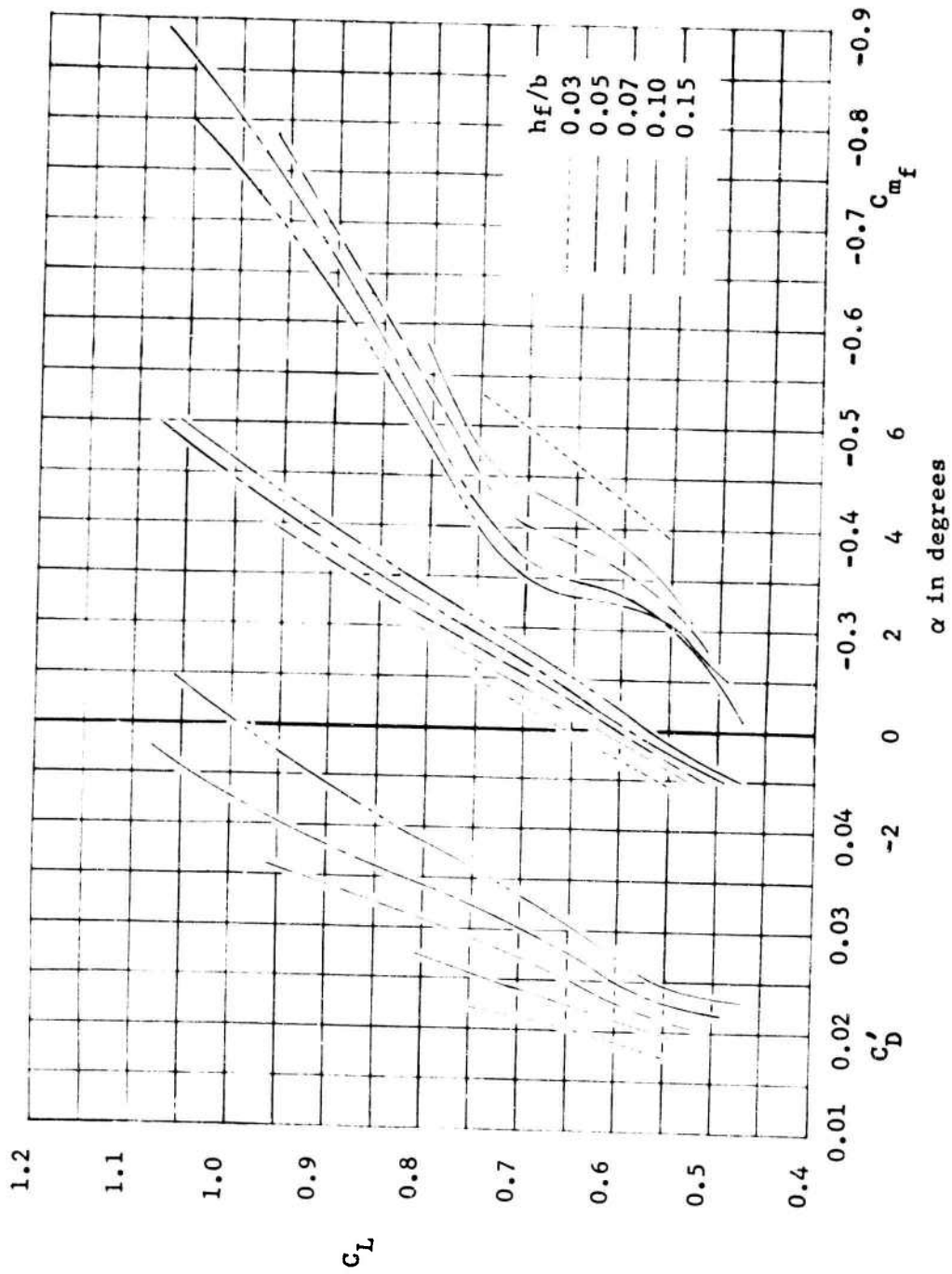


Figure 4 - Longitudinal Aerodynamic Characteristics of the  
 TWIG Model With  $i_{wf} = i_{wa} = 2^\circ$   
 (a) Forward c.g.

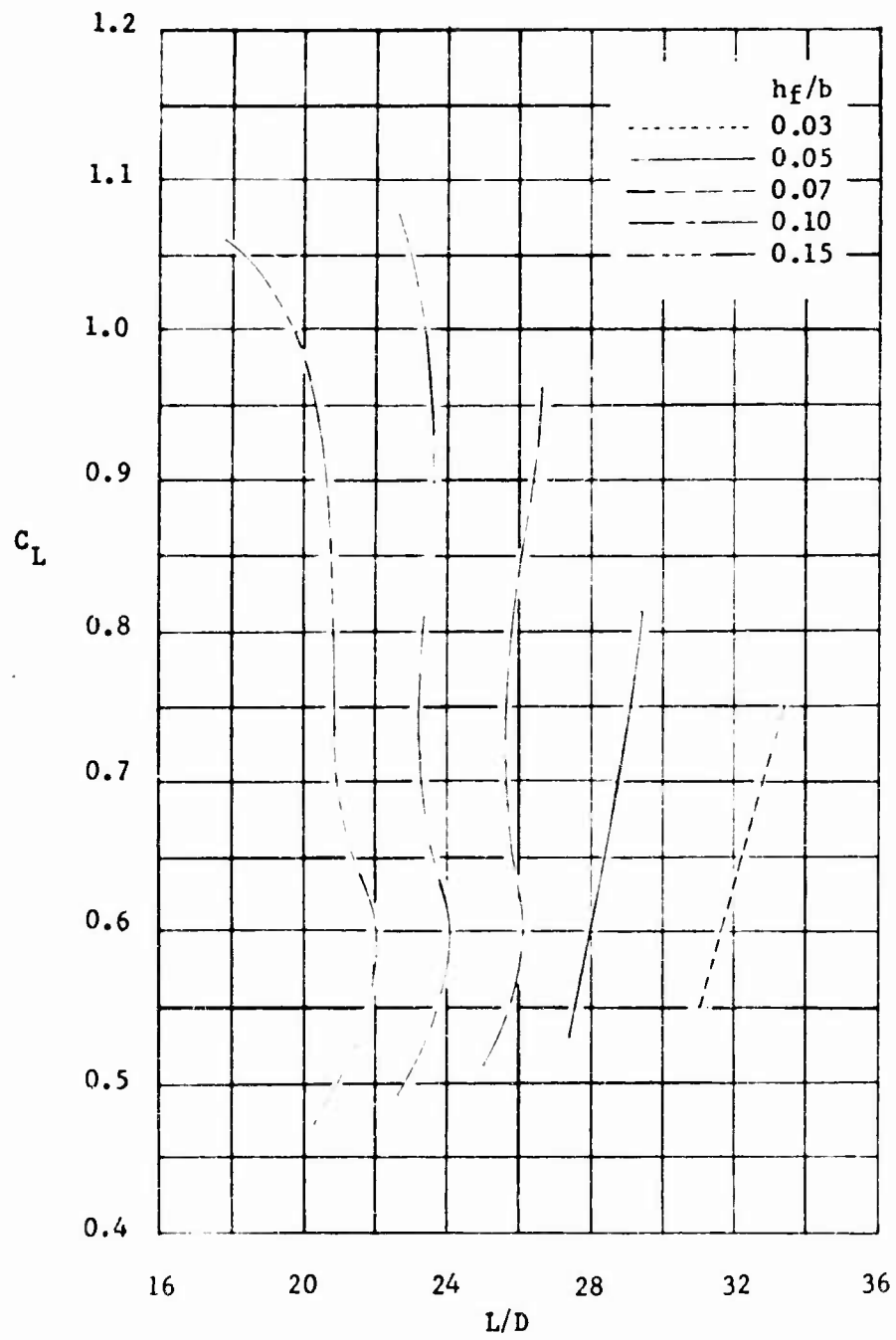


Figure 4 (Continued)

(a) Concluded

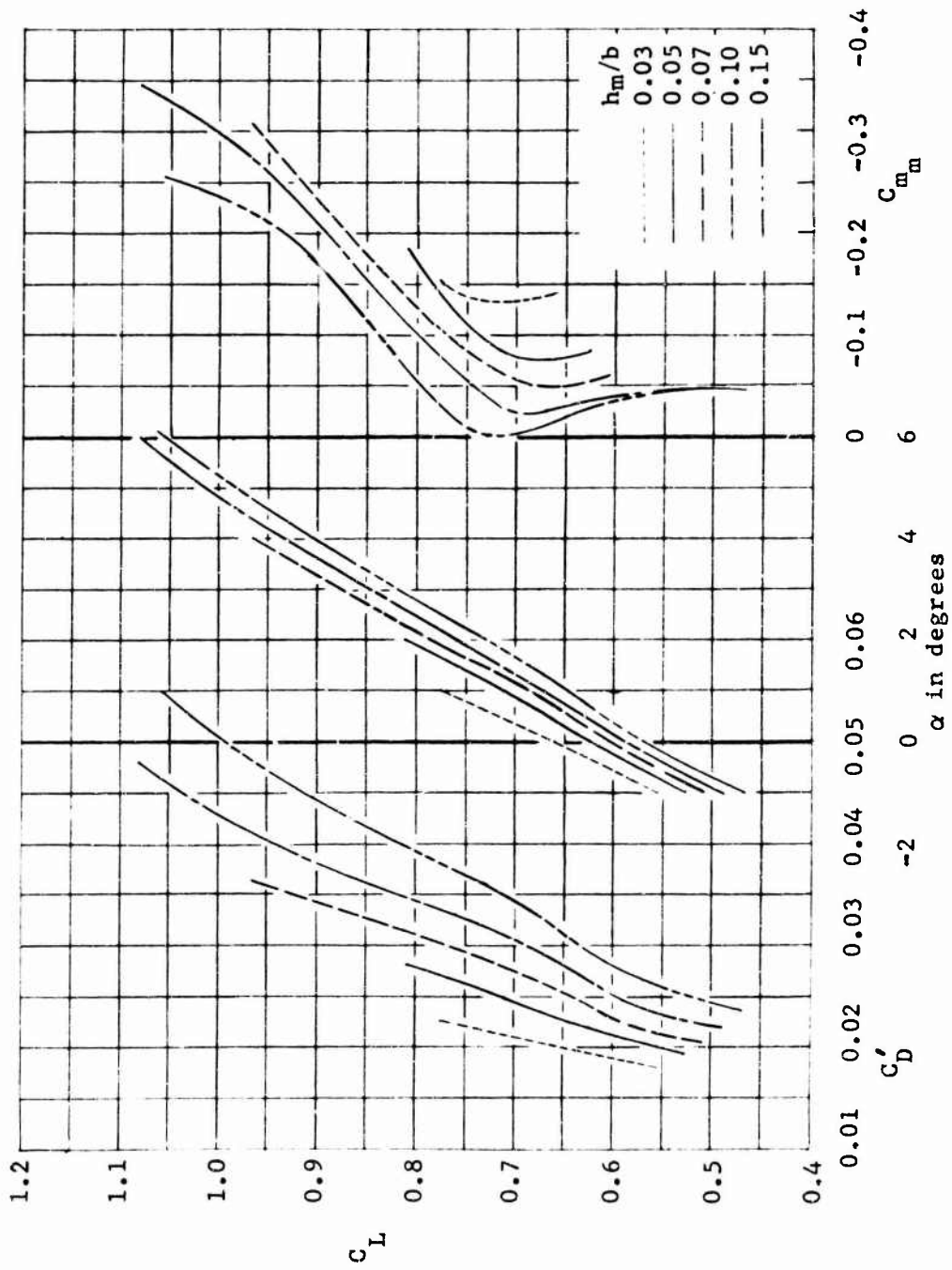


Figure 4 (Continued)  
 (b) Mid c.g.



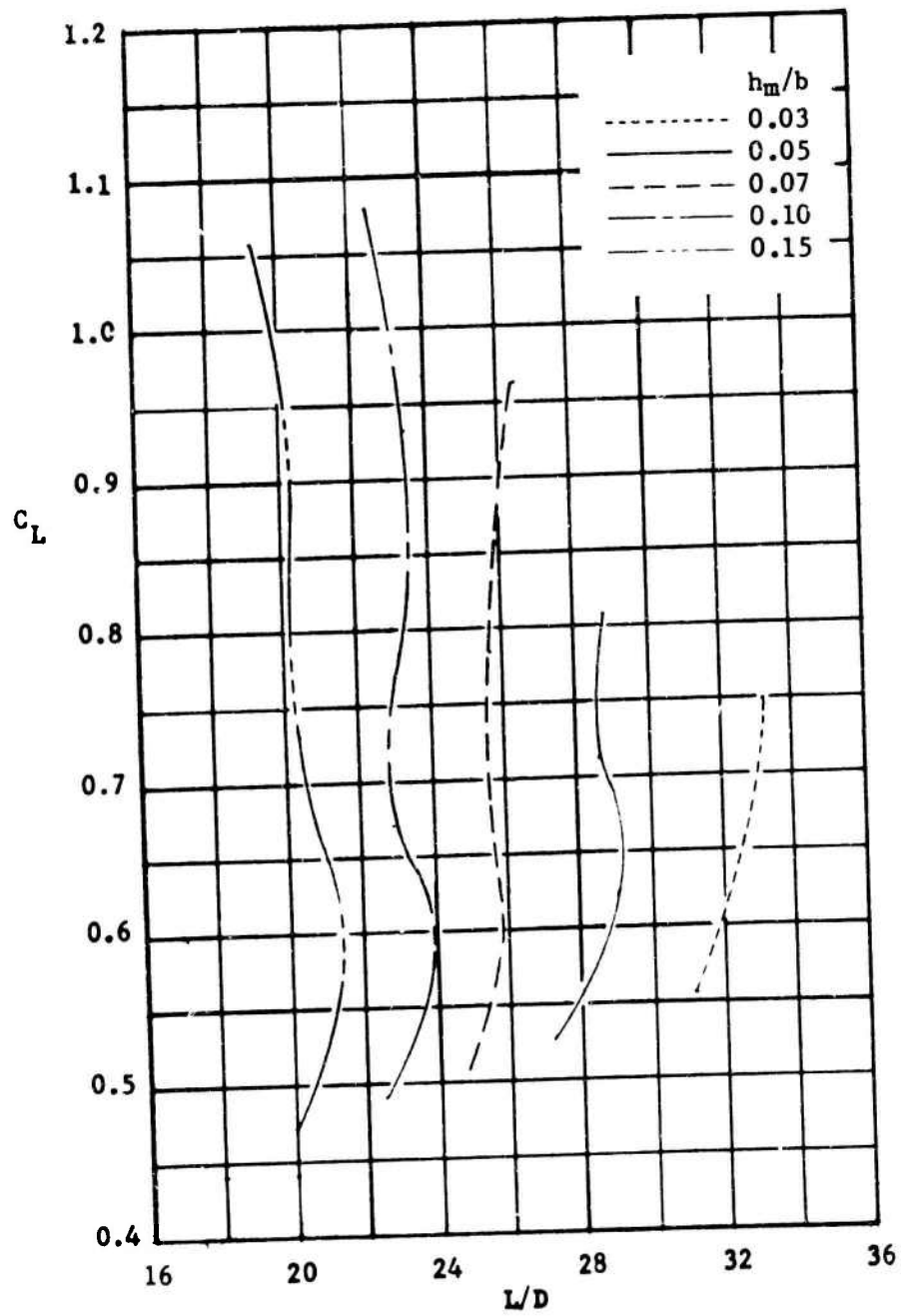


Figure 4 (Continued)  
 (b) Concluded

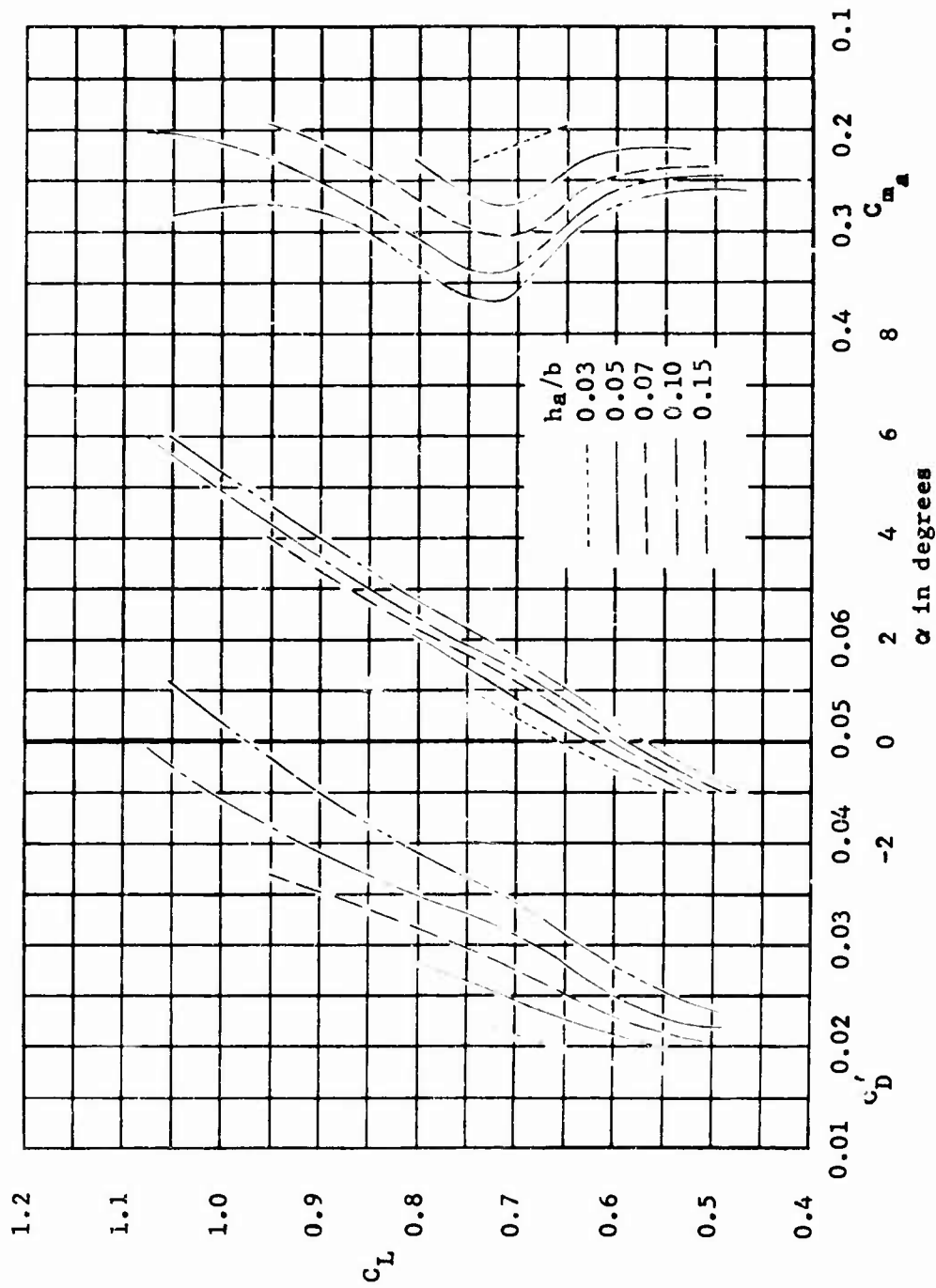


Figure 4 (Continued)

(c) Aft c.g.

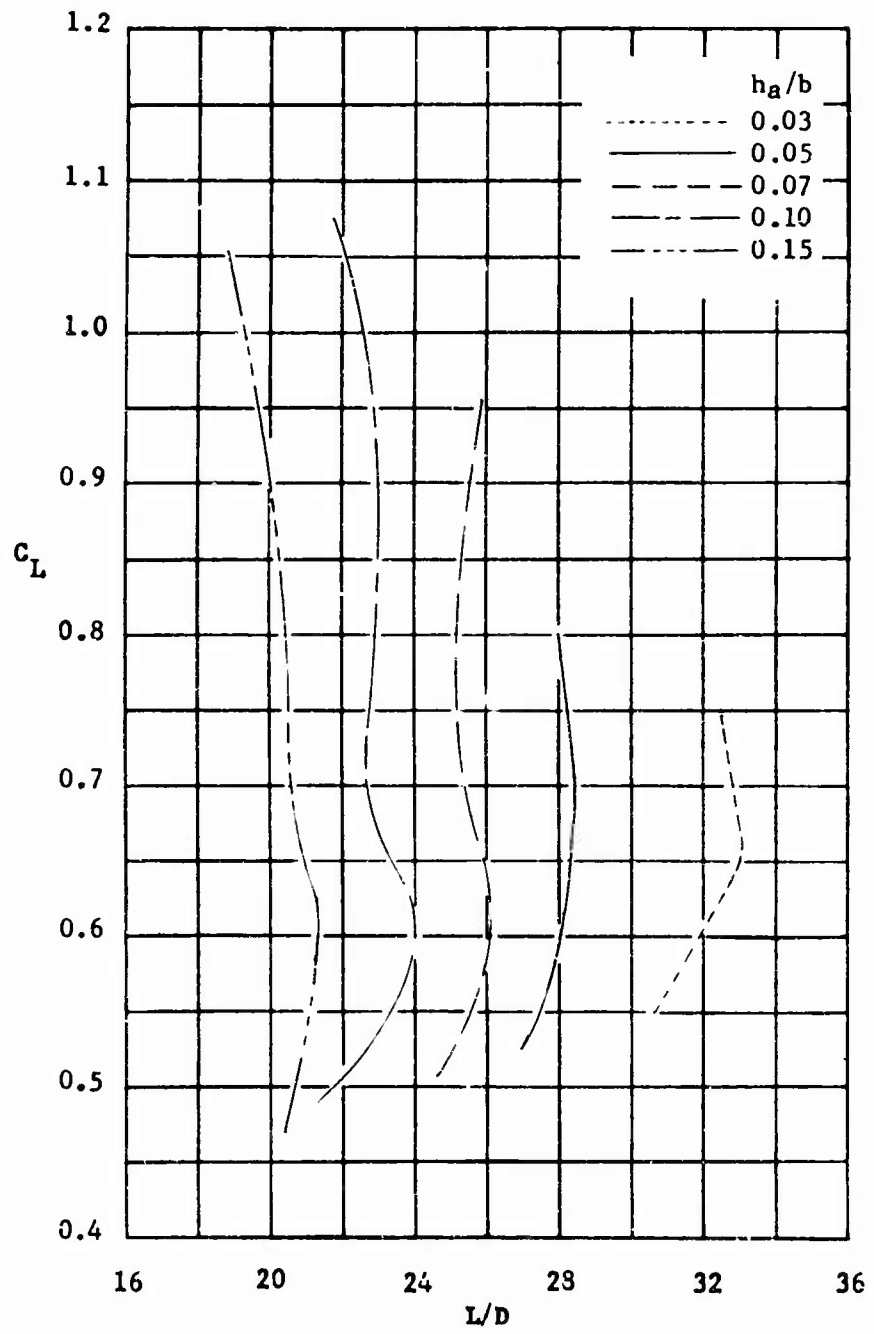


Figure 4 (Concluded)

(c) Concluded

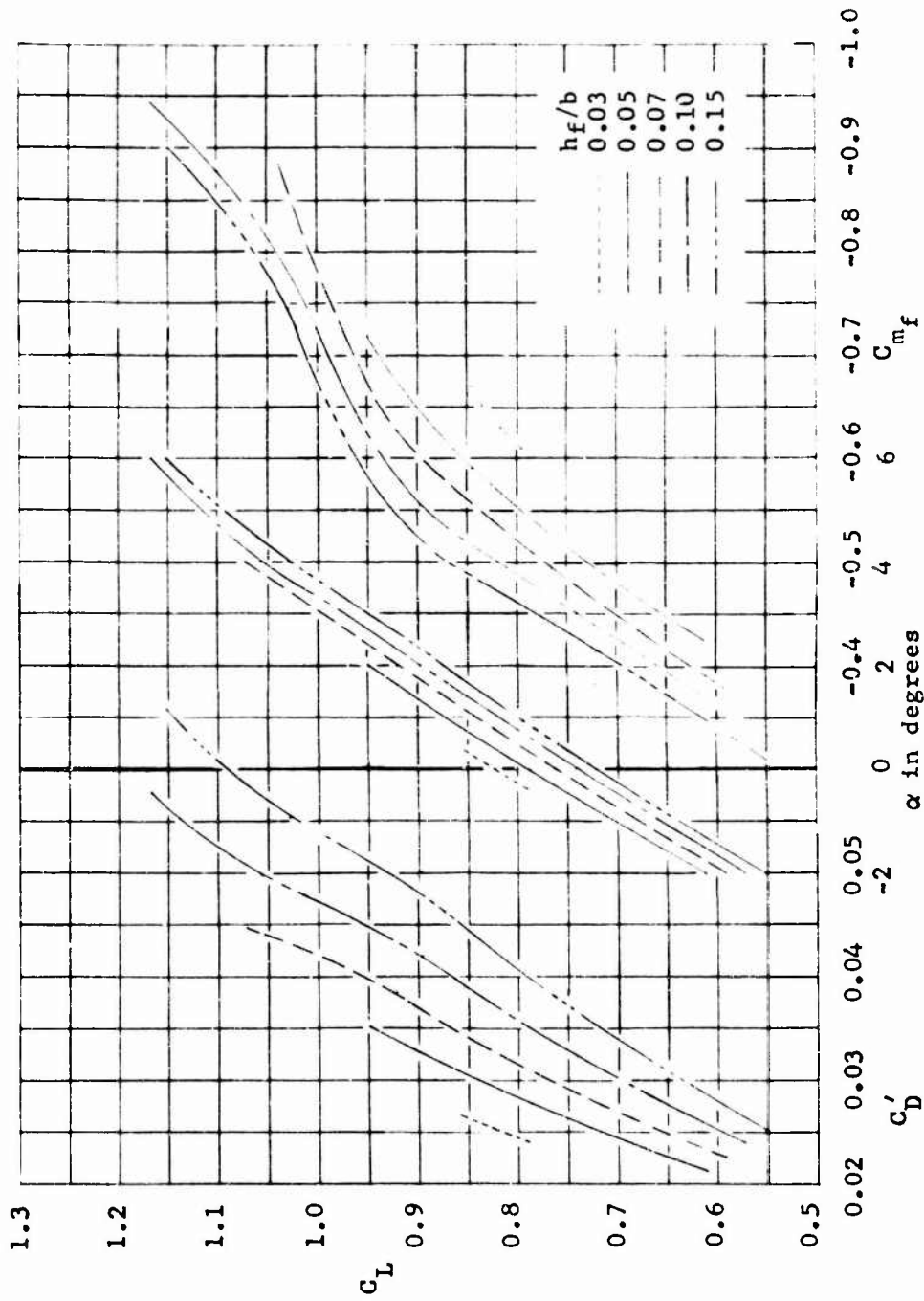


Figure 5 - Longitudinal Aerodynamic Characteristics of the

TWIG Model With  $i_{w_f} = i_{w_a} = 4^\circ$

(a) Forward c.8.

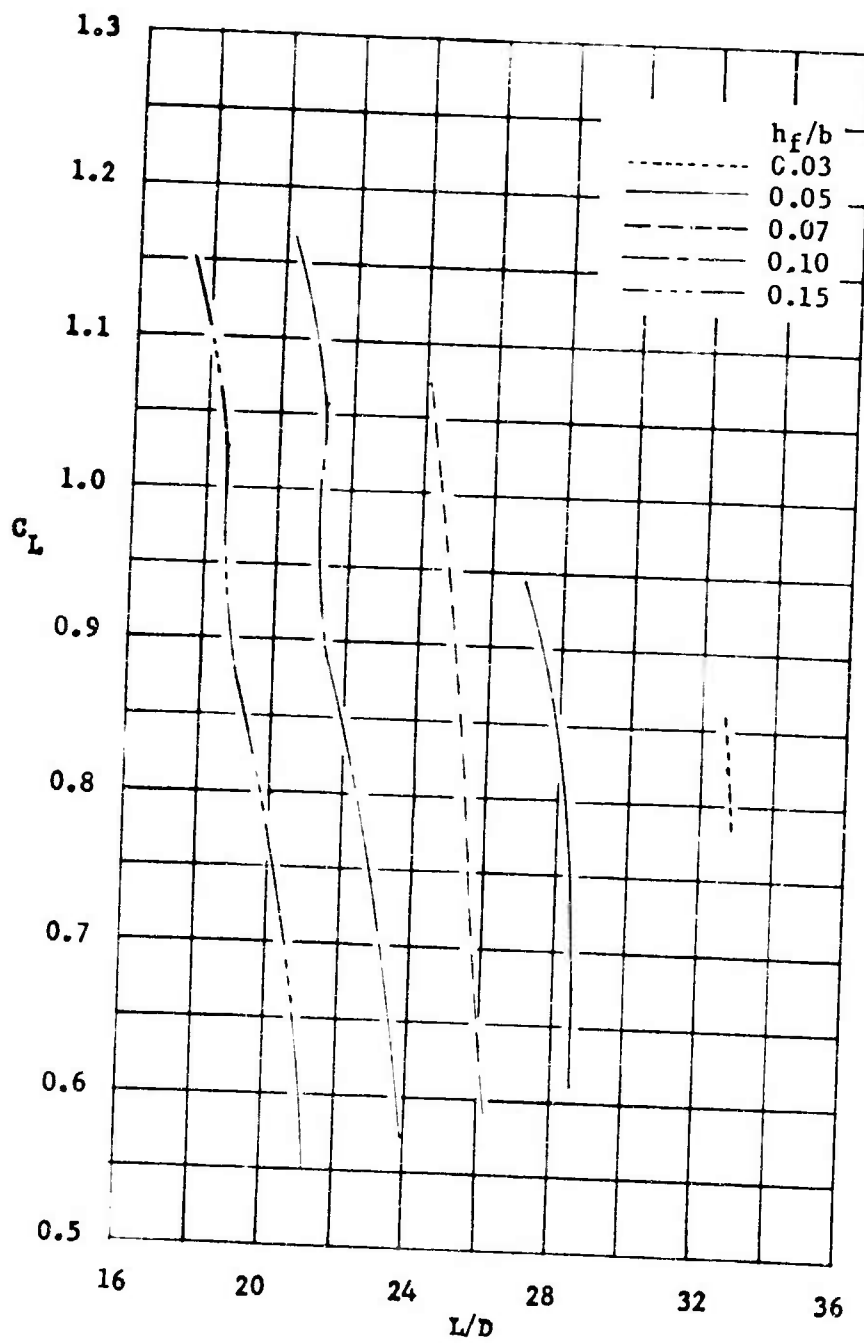


Figure 5 (Continued)

(a) Concluded

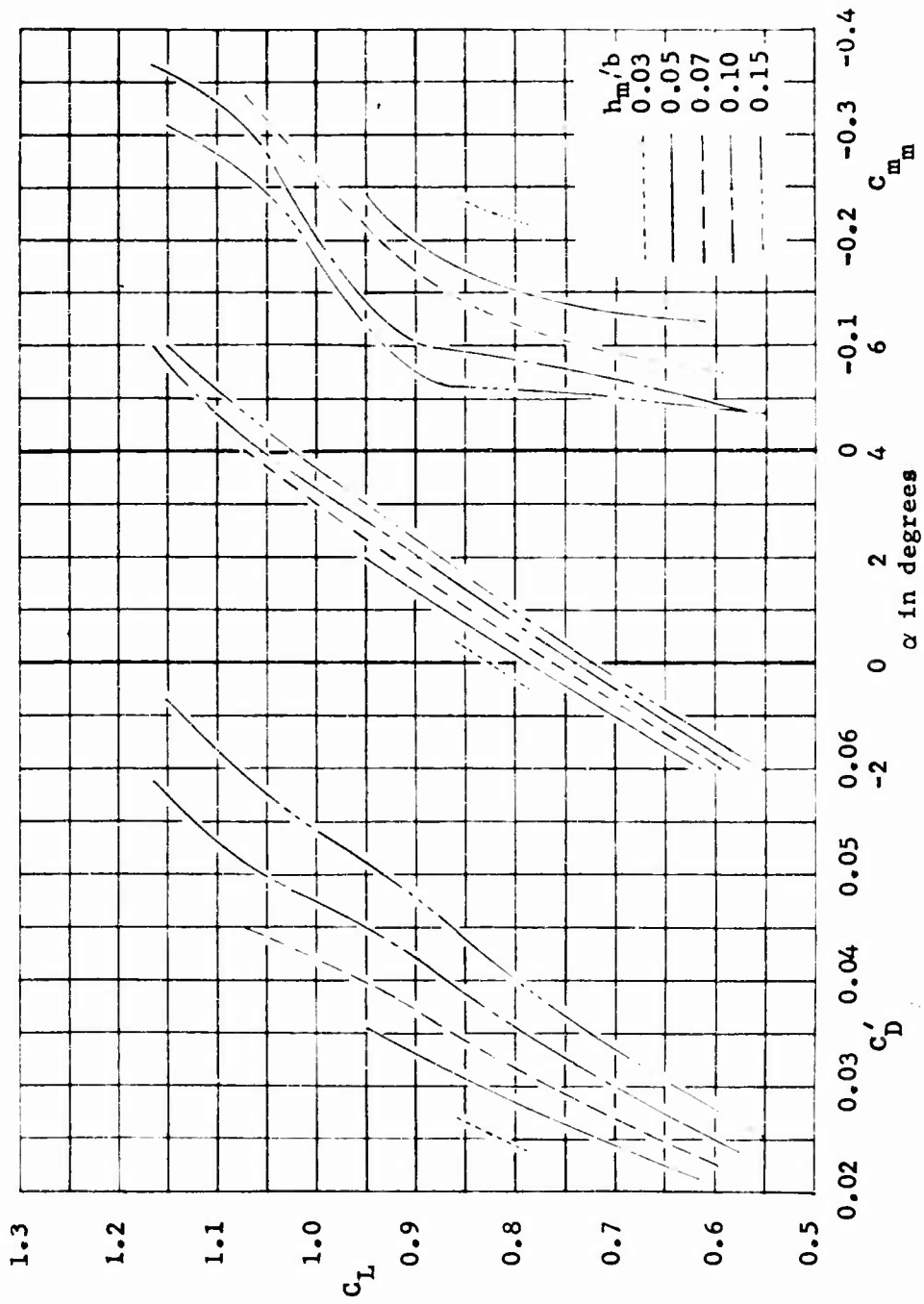


Figure 5 (Continued)

(b) Mid c.g.

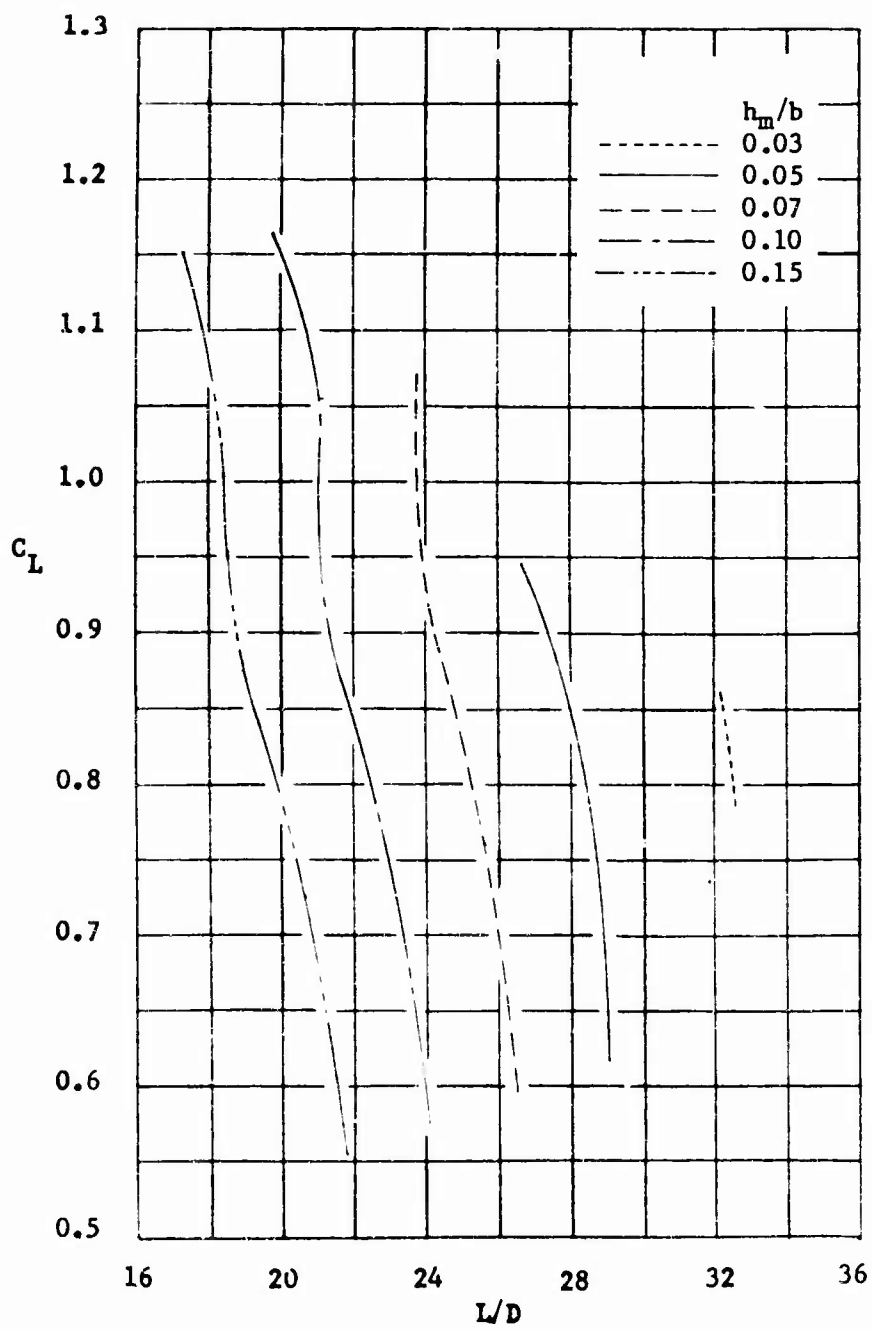


Figure 5 (Continued)

(b) Concluded

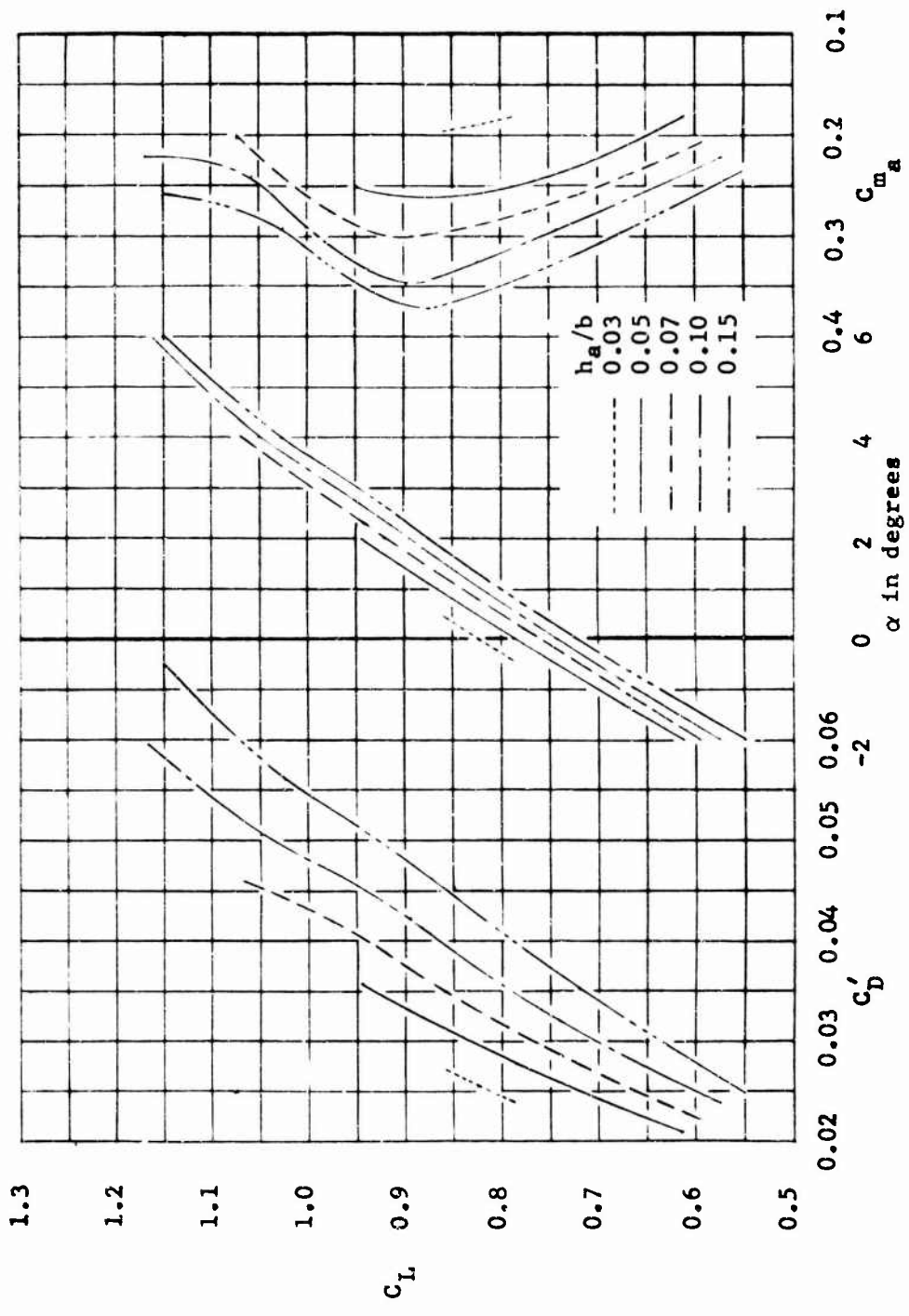


Figure 5 (Continued)  
(c) Aft c-8.



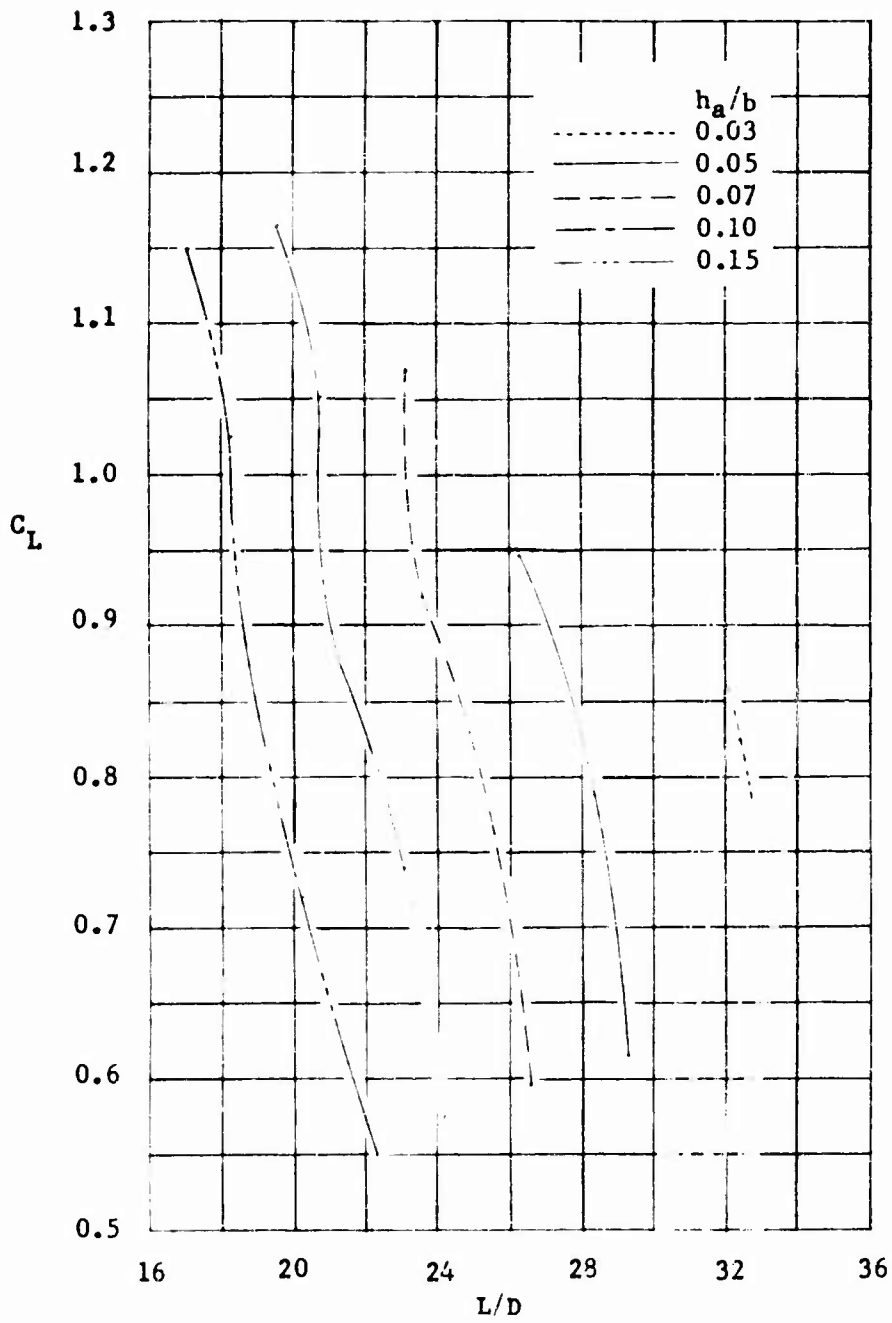


Figure 5 (Concluded)

(c) Concluded

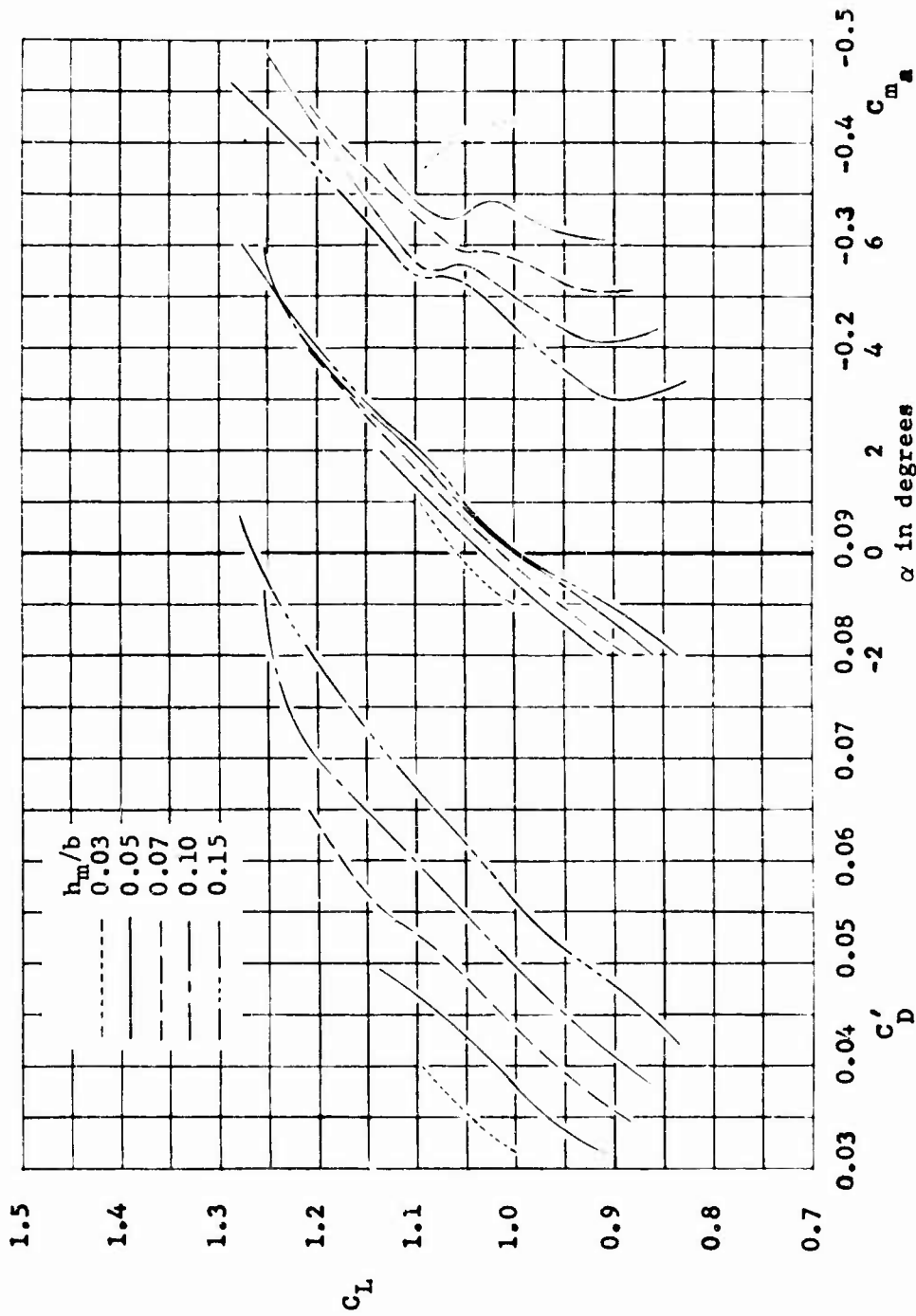


Figure 6 - Longitudinal Aerodynamic Characteristics of the

TWIG Model With  $i_{wf} = i_{wa} = 8^\circ$

(a) Mid c.g.

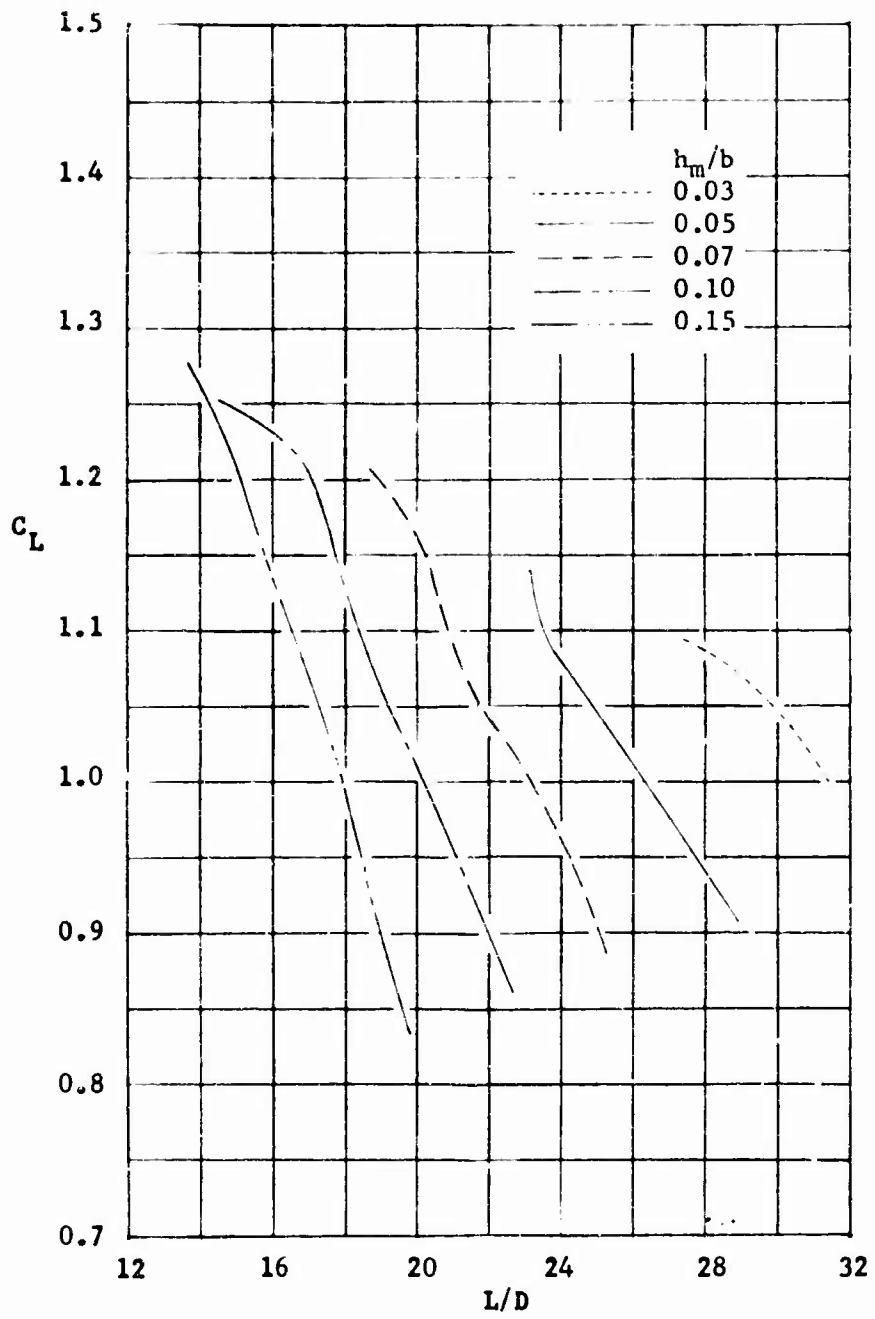


Figure 6 (Continued)

(a) Concluded

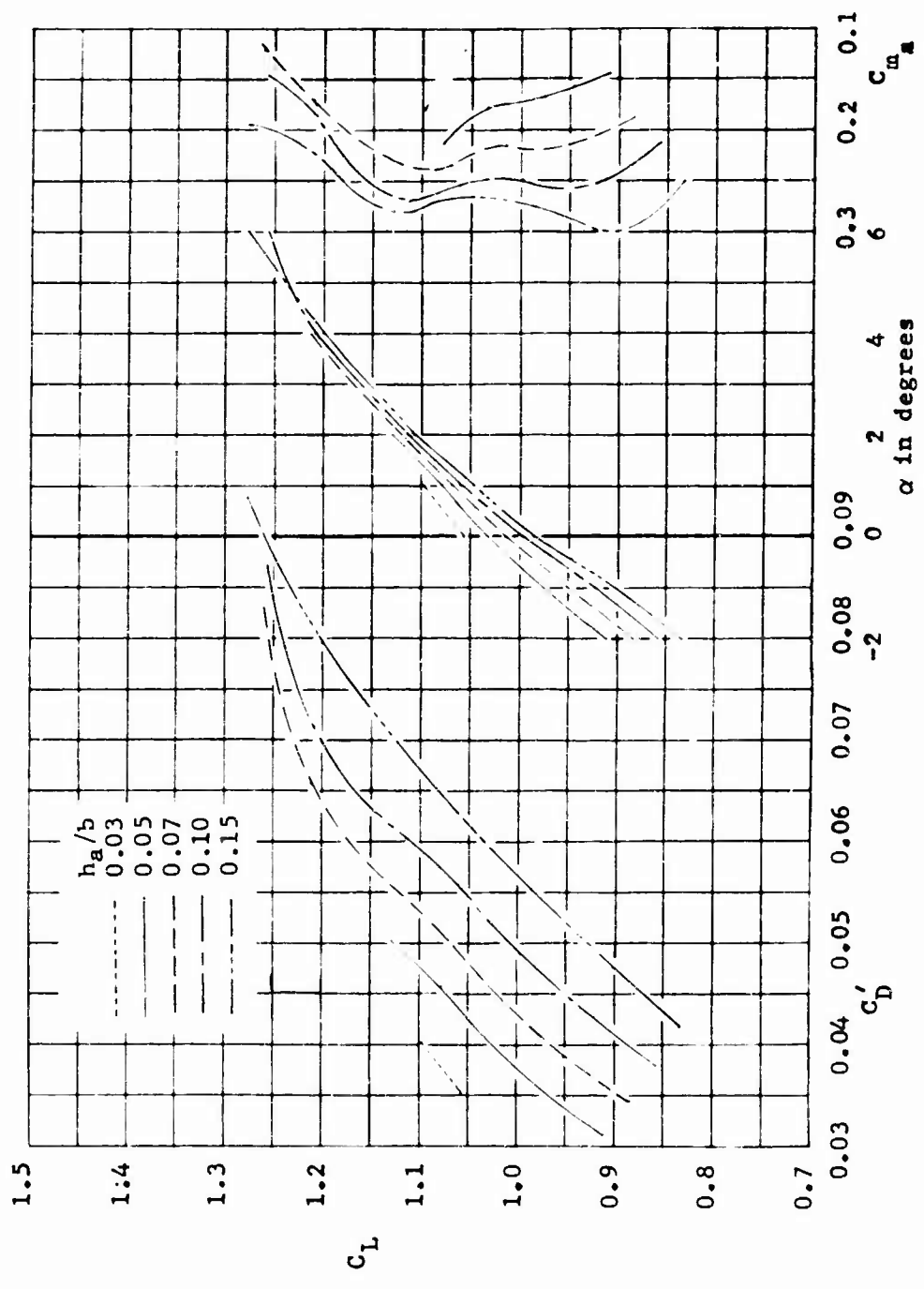


Figure 6 (Continued)  
 (b) Aft c.g.

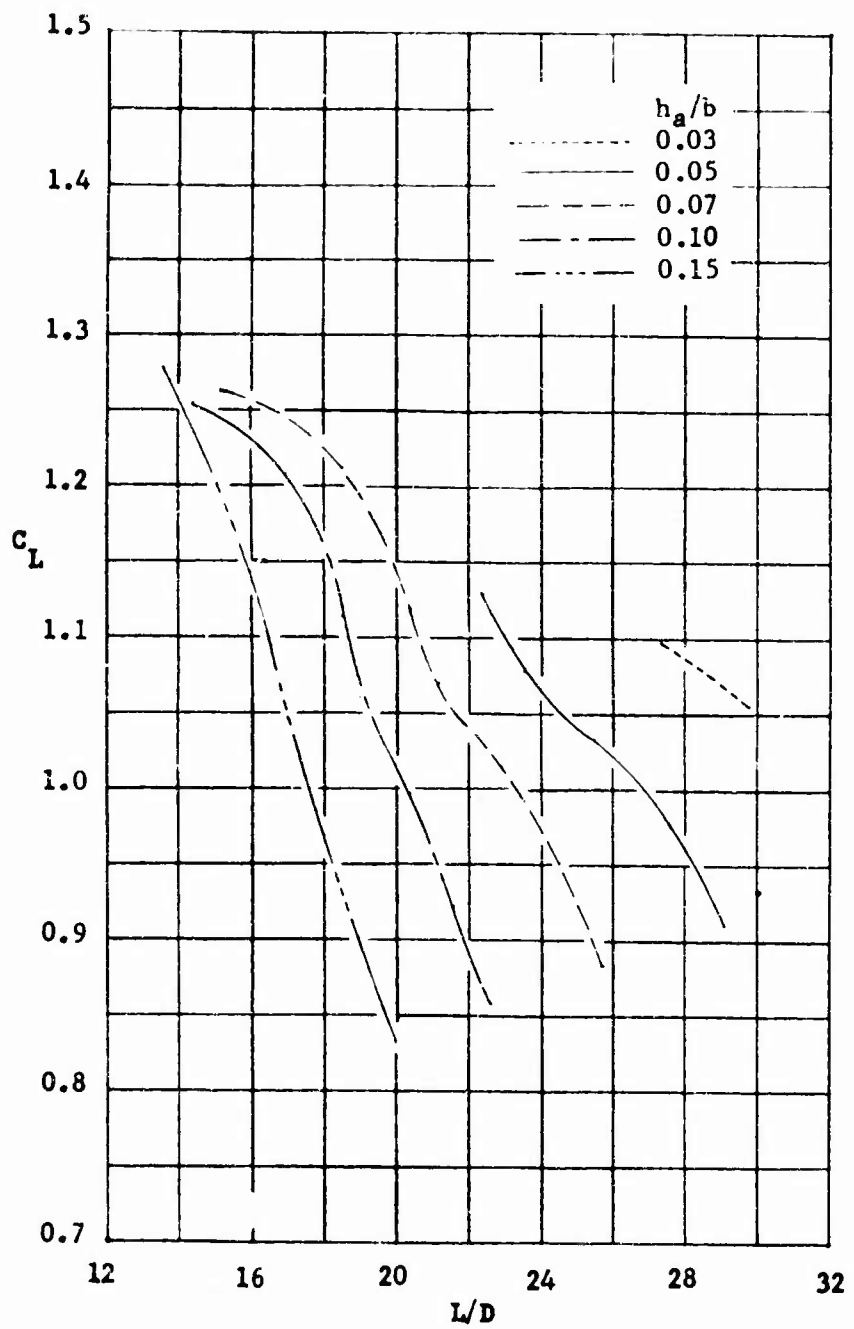


Figure 6 (Concluded)

(b) Concluded

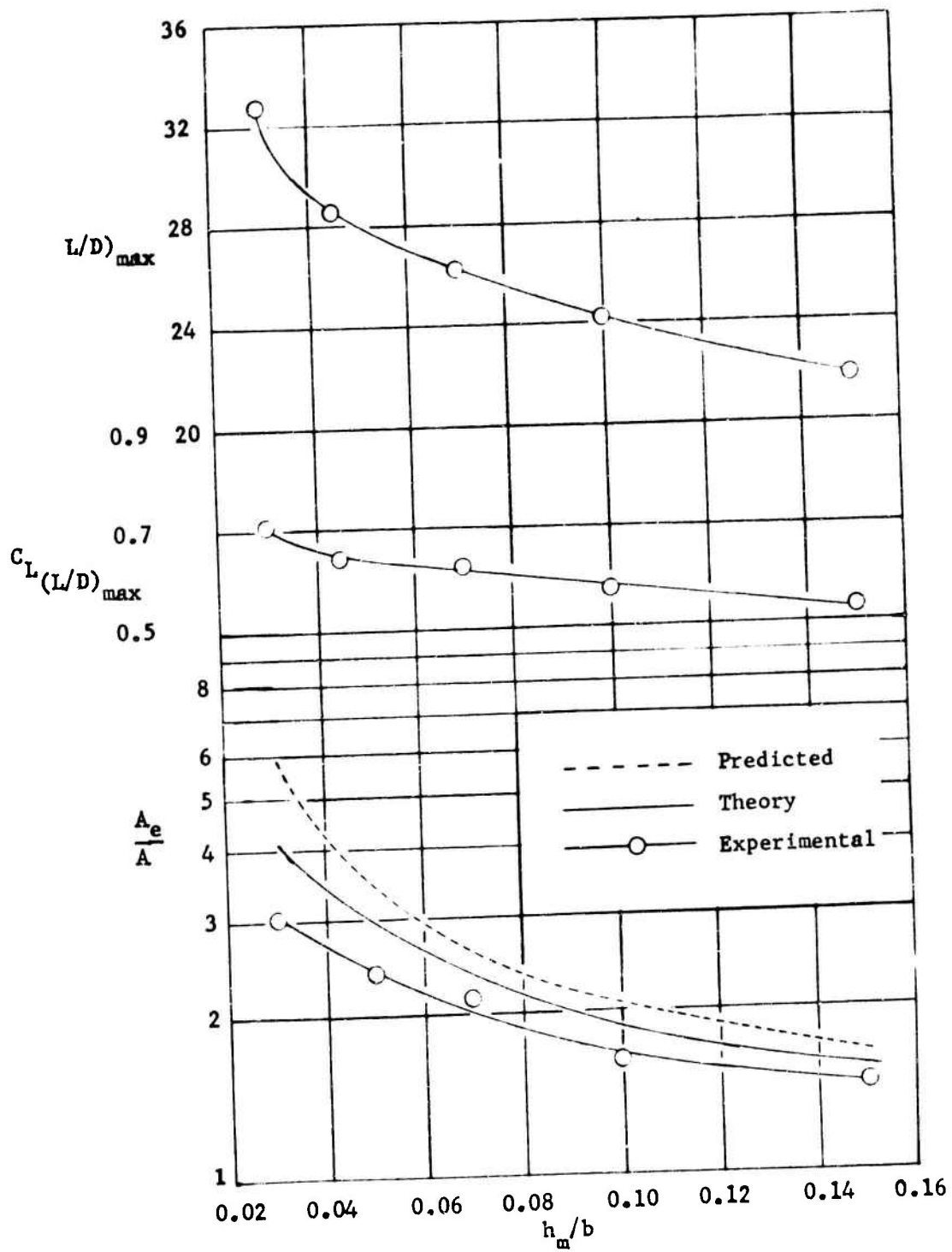


Figure 7 - Performance Parameters of Trimmed TWIG Model at Mid c.g.  $\alpha = 0^\circ$

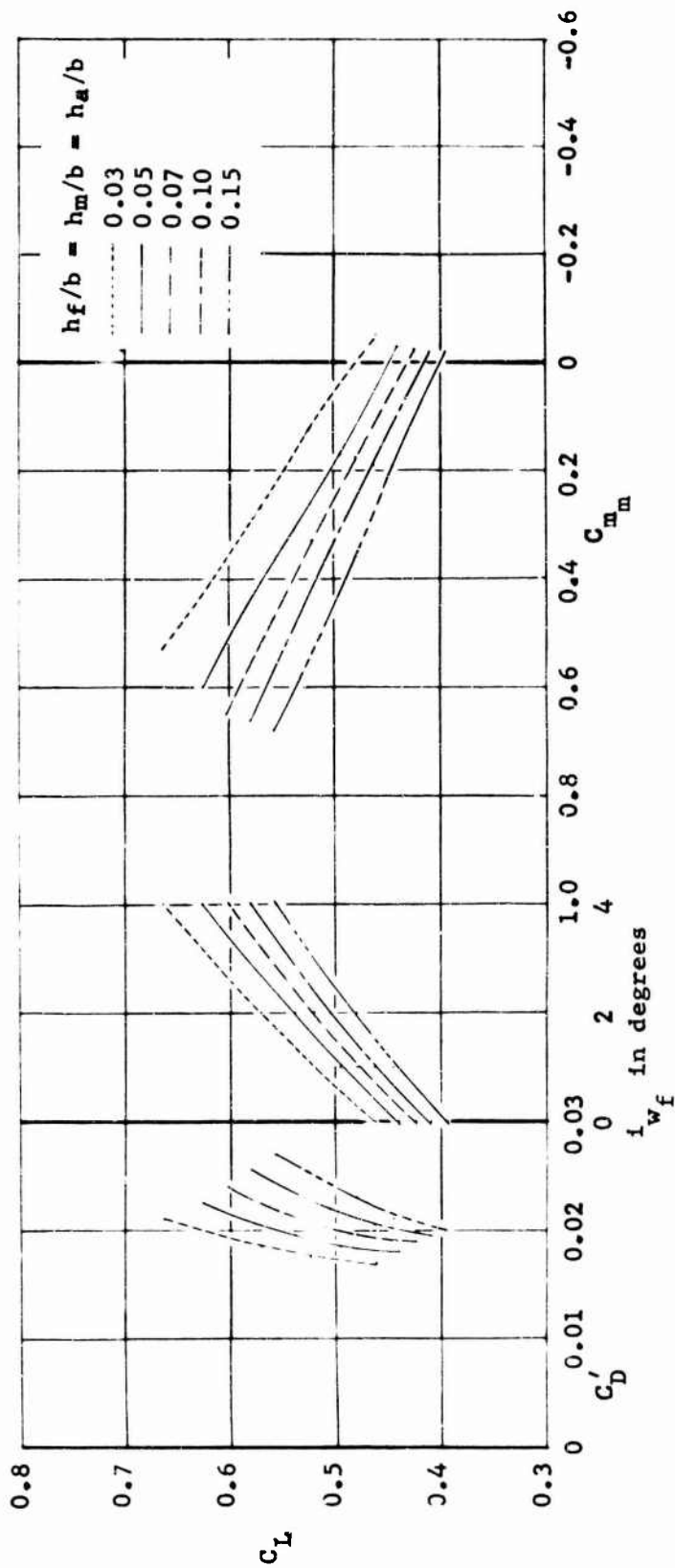


Figure 8 - Forward Wing Effectiveness of the TWIG Model With  
 a Mid c.g. Location and  $i_{wg} = \alpha = 0^\circ$

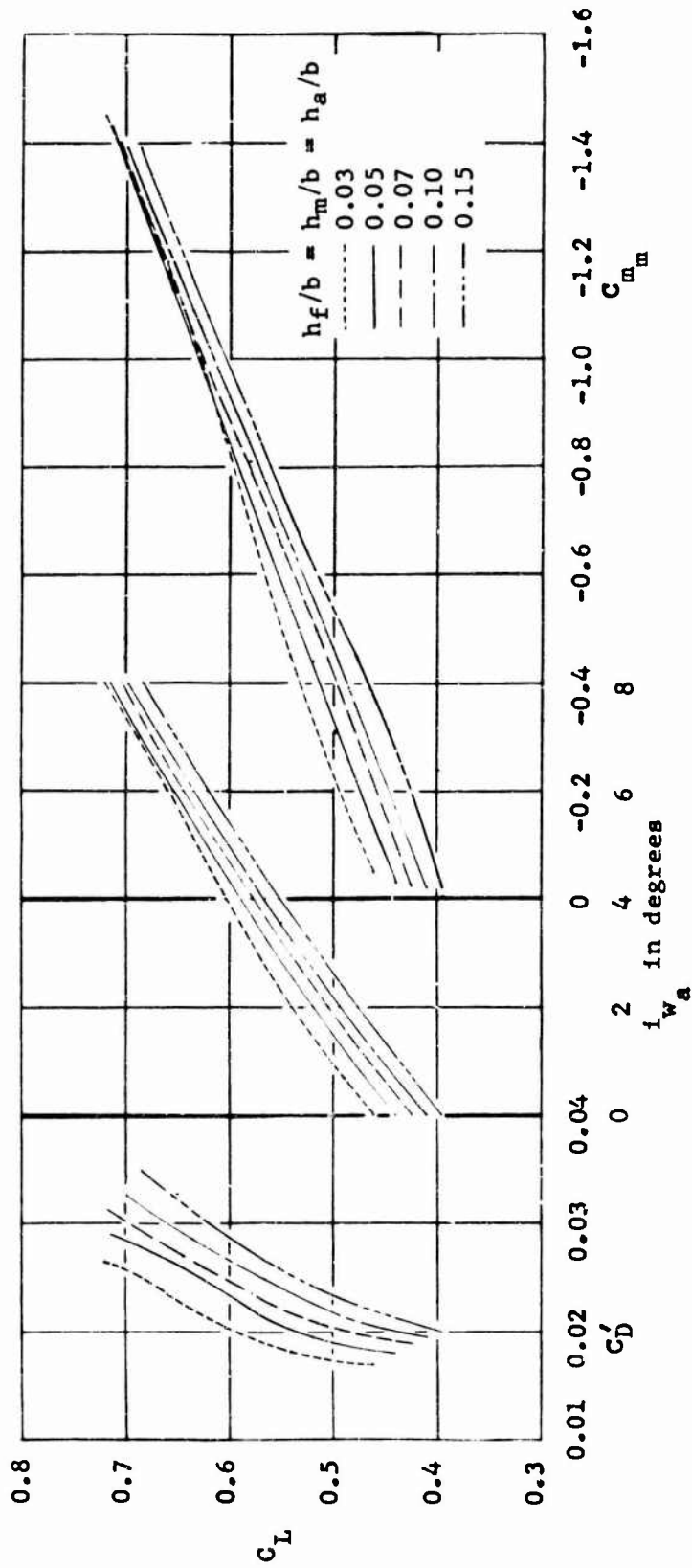


Figure 9 - Aft Wing Effectiveness of the TWIG Model With a

Mid c.g. Location and  $i_{w_f} = \alpha = 0^\circ$



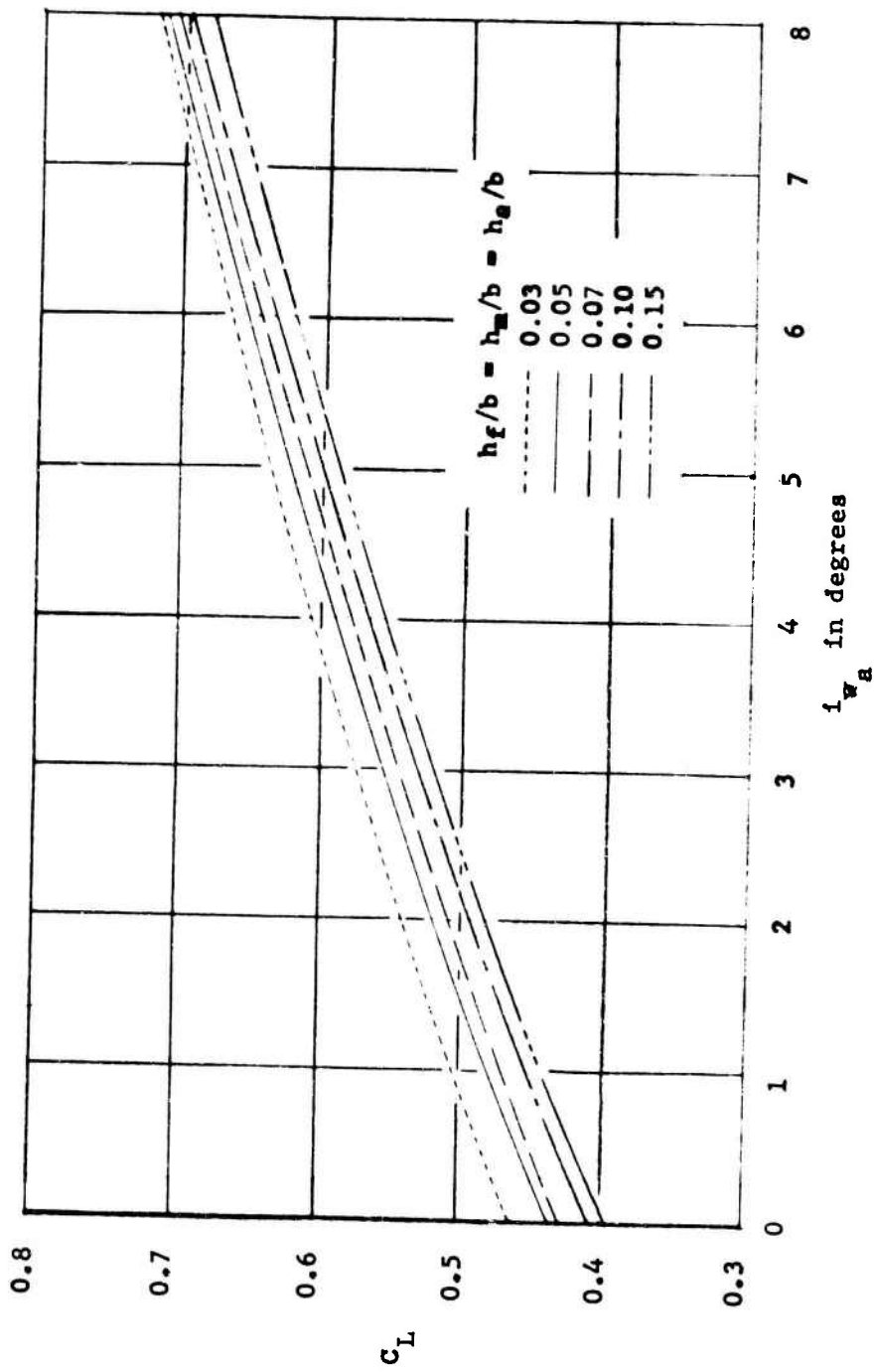


Figure 10 - Effect of  $i_{w_a}$  on the TWIG Model Lift Performance With  $\alpha = 0^\circ$

(a)  $i_{w_f} = 0^\circ$

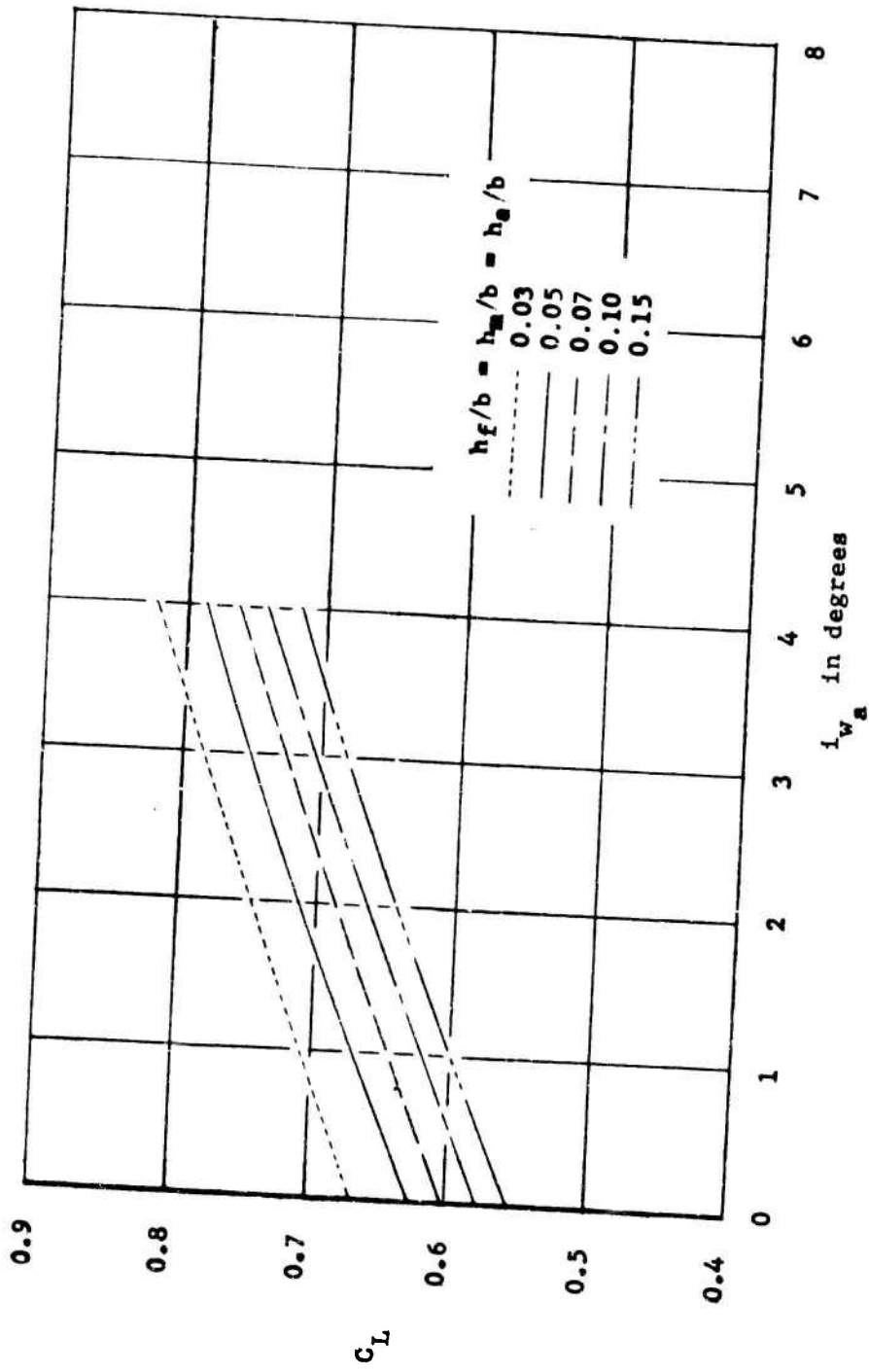


Figure 10 (Continued)

(b)  $i_{w_f} = 4^\circ$

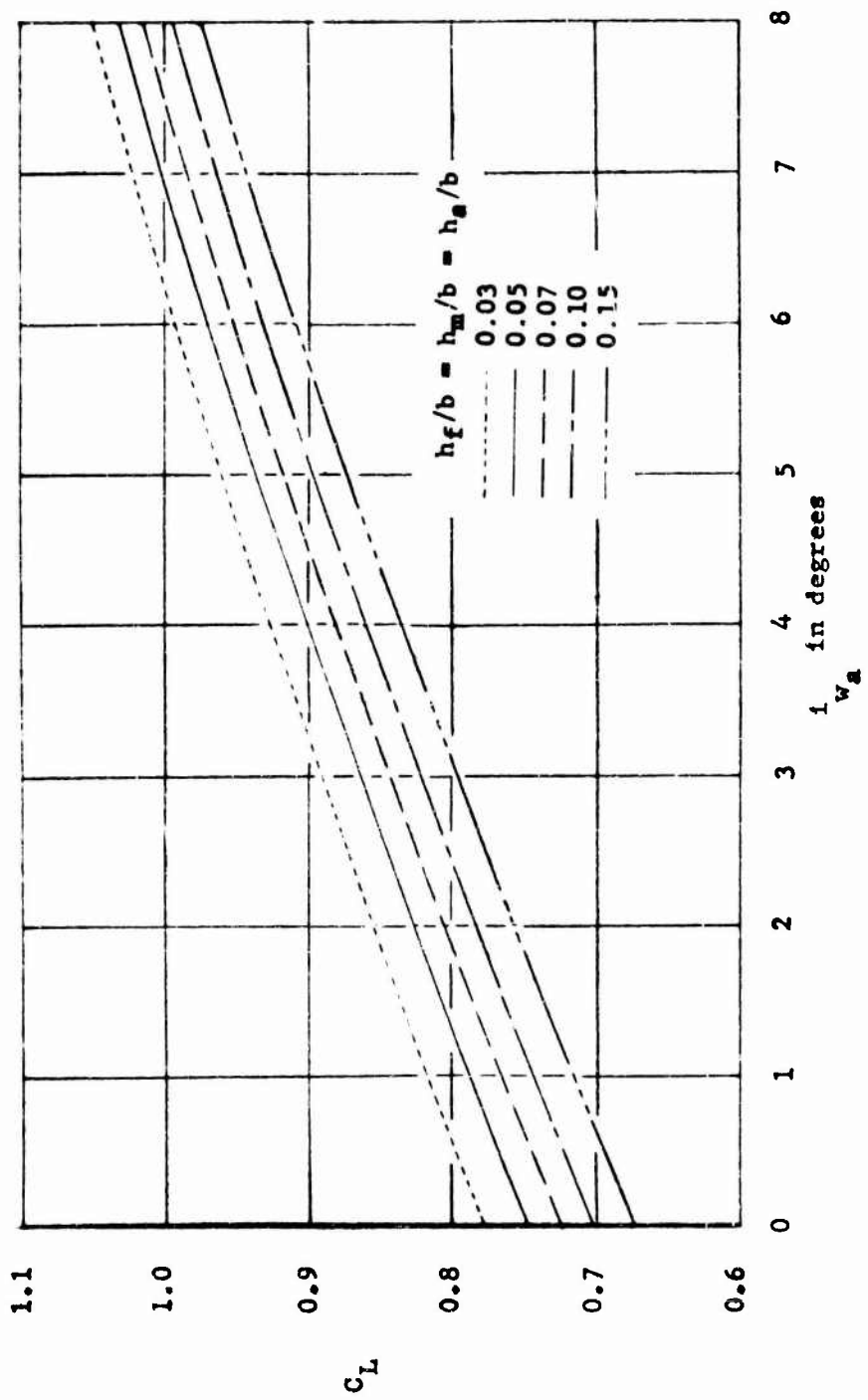


Figure 10 (Concluded)  
 (c)  $i_{w_f} = 8^\circ$

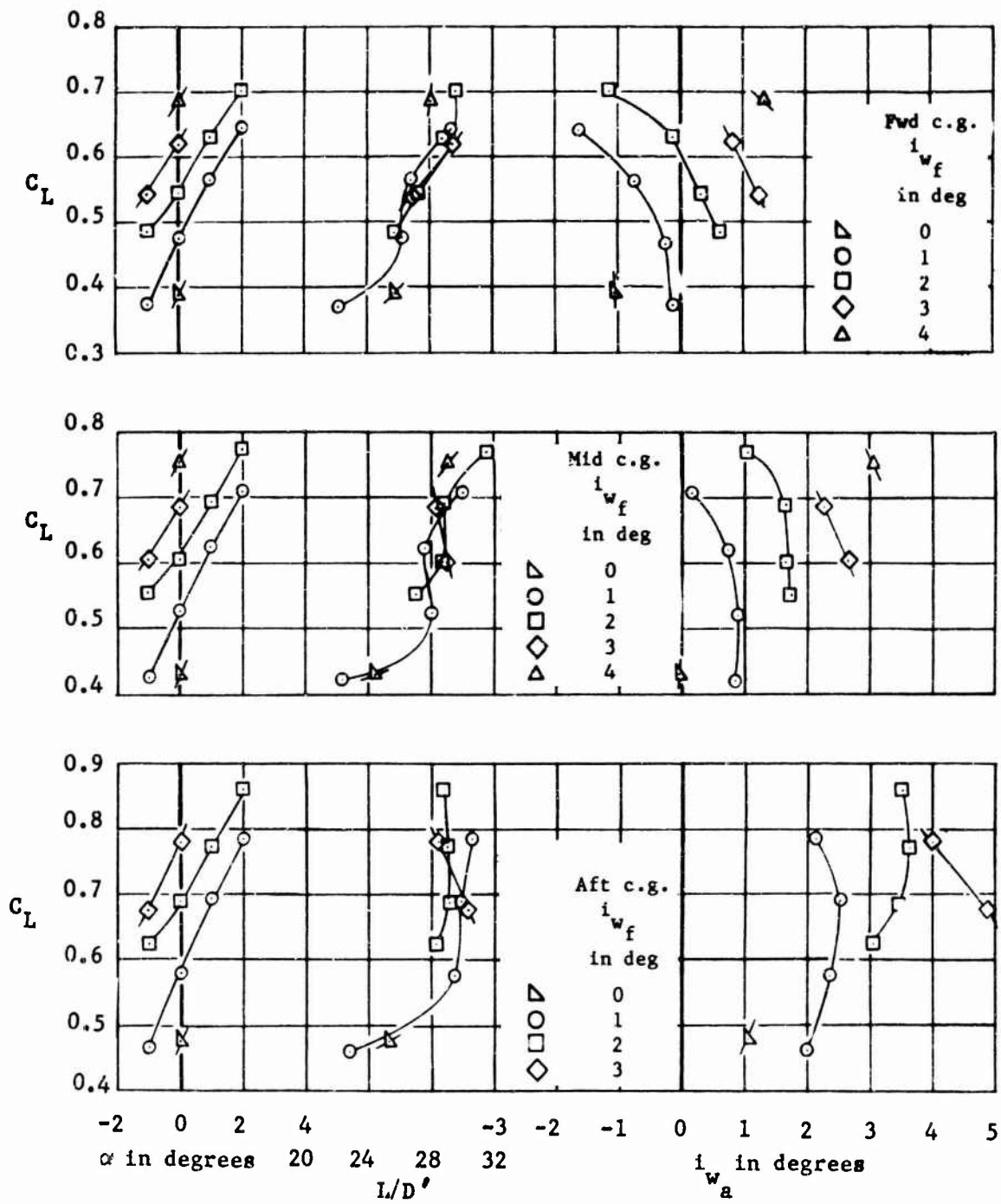


Figure 11 - Required  $i_{wa}$  for Trim of the TWIG Model In Ground Effect

(a)  $h/b = 0.05$

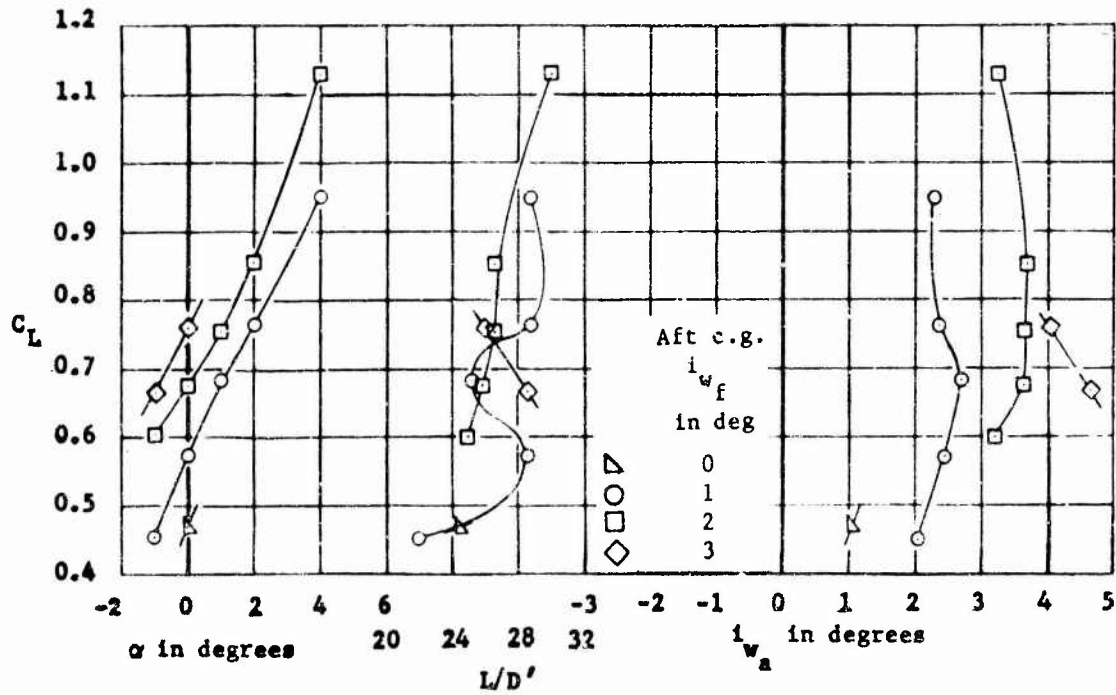
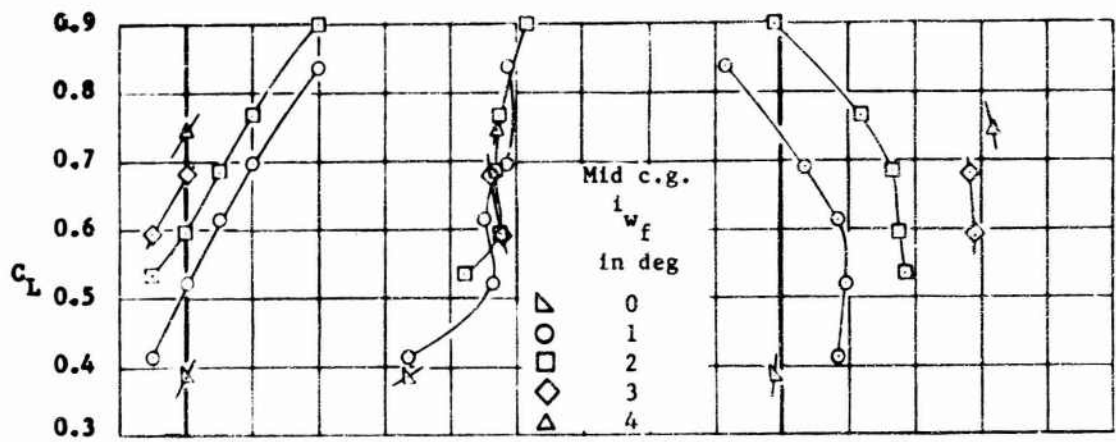
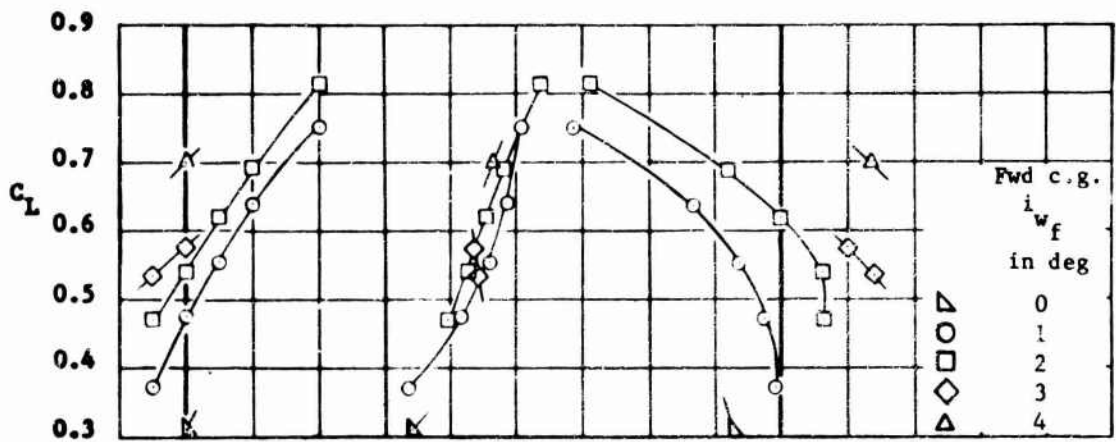


Figure 11 (Continued)  
 (b)  $h/b = 0.063$

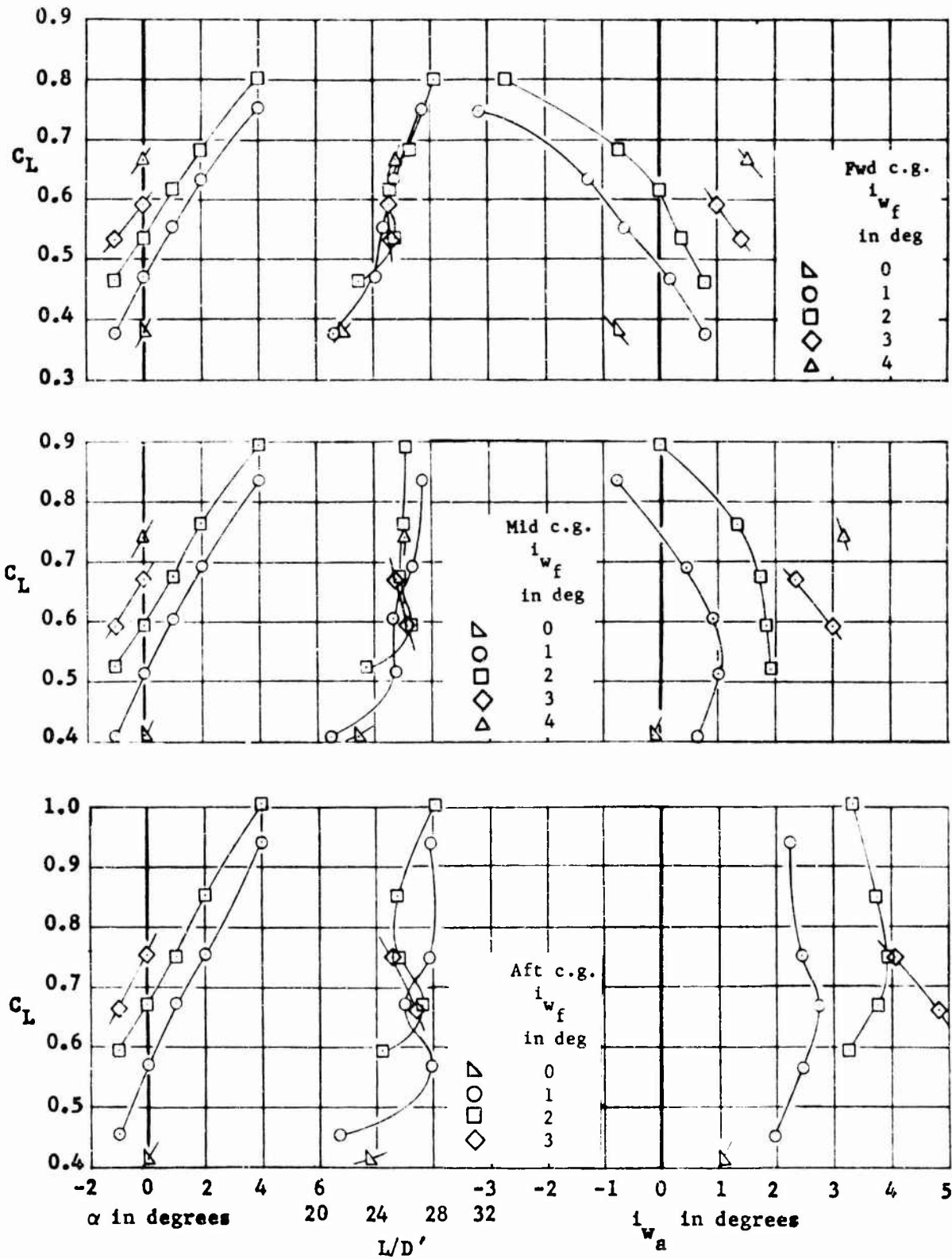


Figure 11 (Continued)

(c)  $h/b = 0.07$

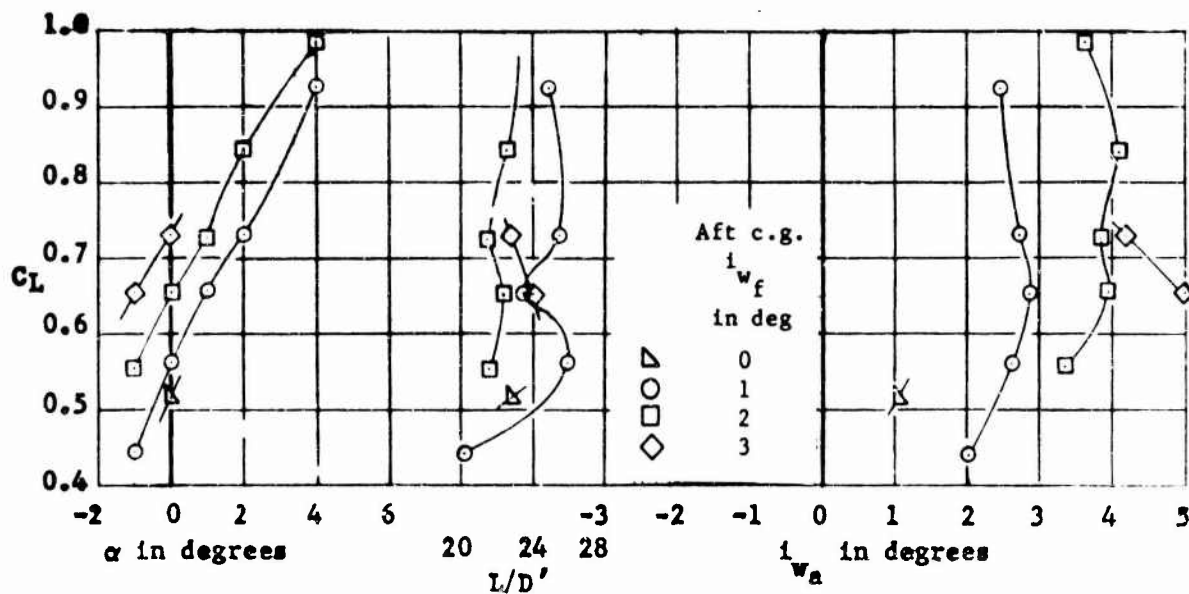
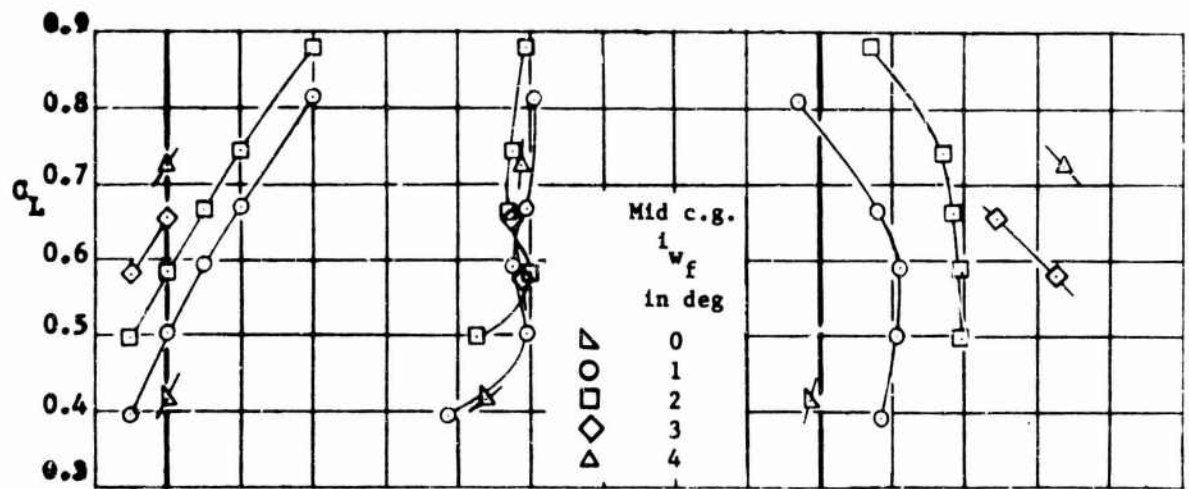
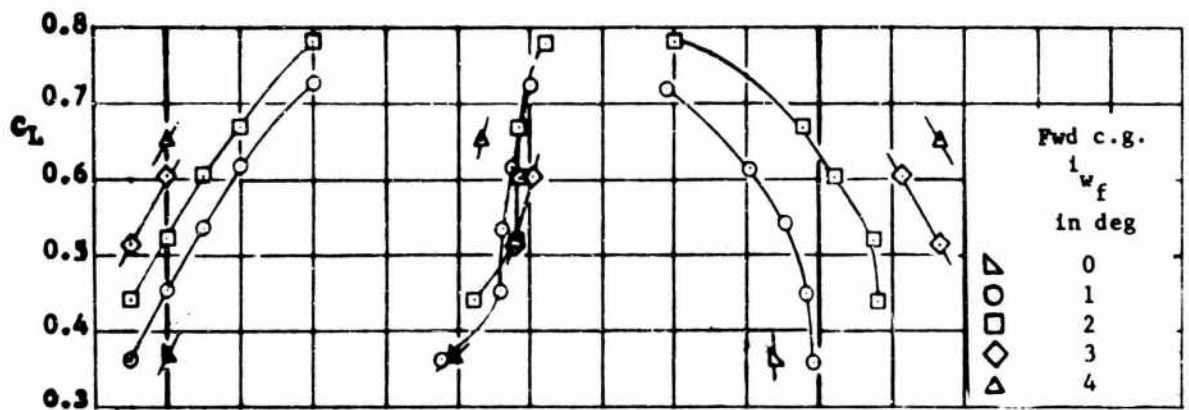


Figure 11 (Continued)

(d)  $h/b = 0.10$

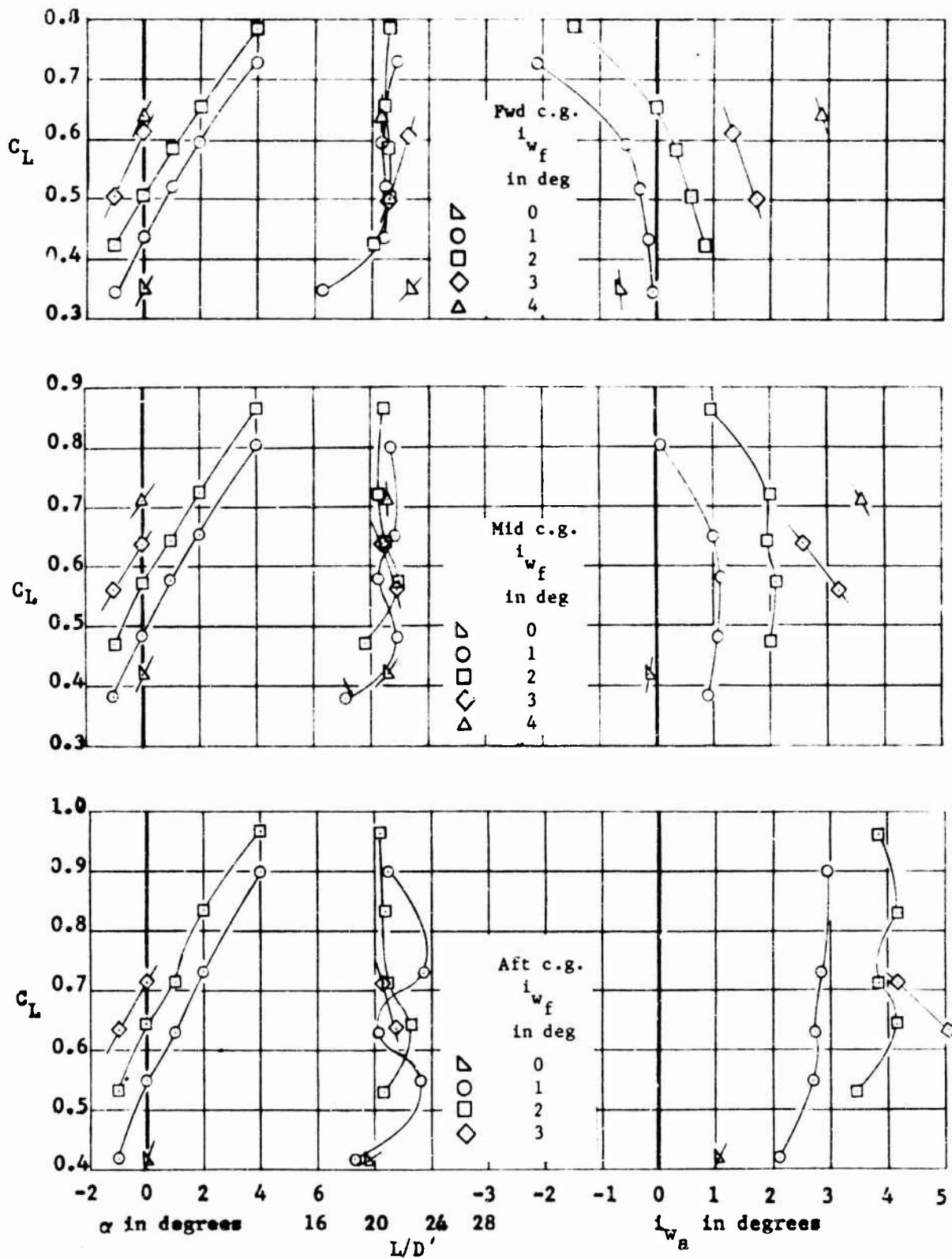


Figure 11 (Concluded)

(e)  $h/b = 0.15$



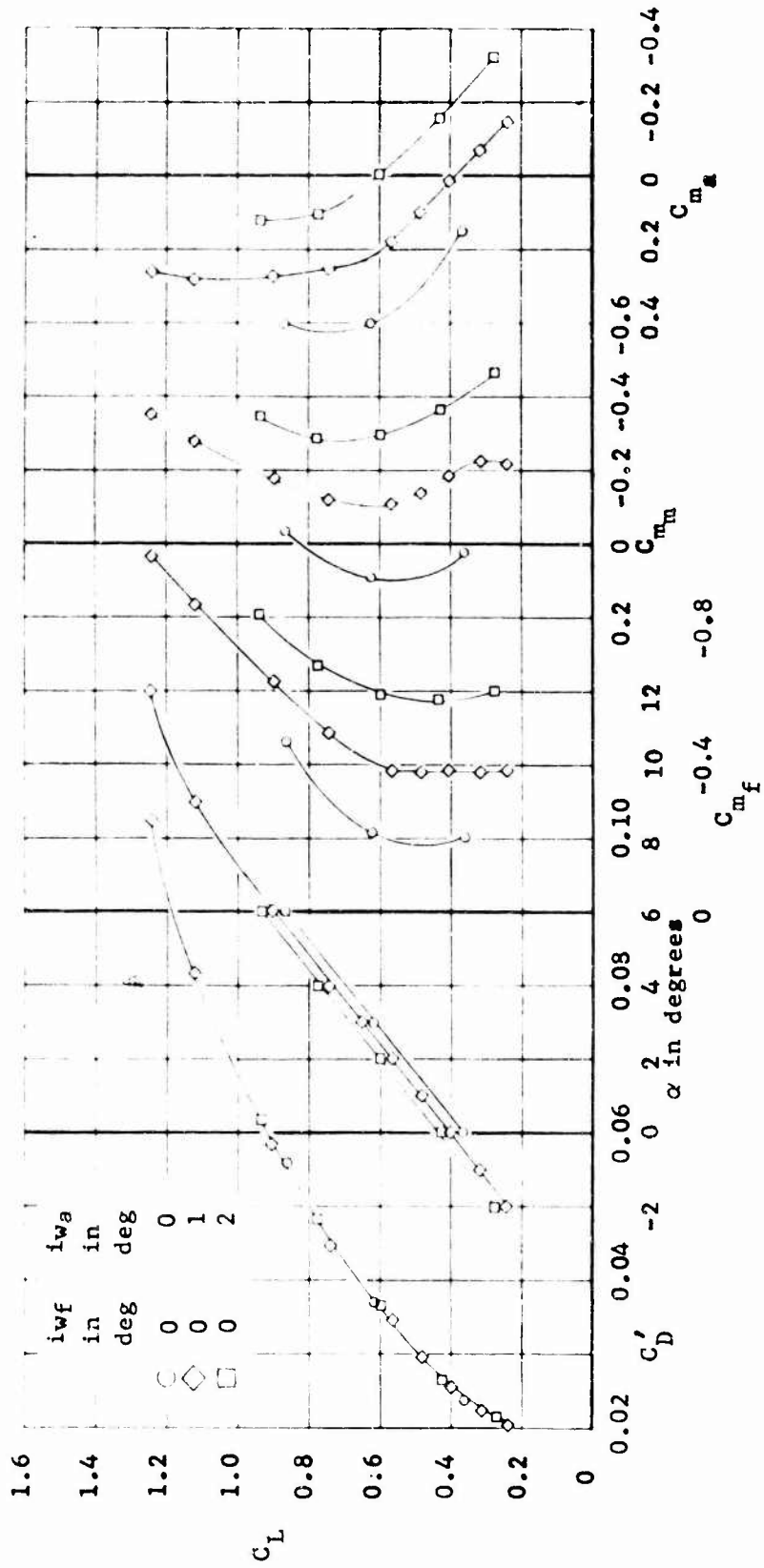


Figure 12 - Longitudinal Aerodynamic Characteristics of the TWIG Model Out of Ground Effect ( $h/b = \infty$ )

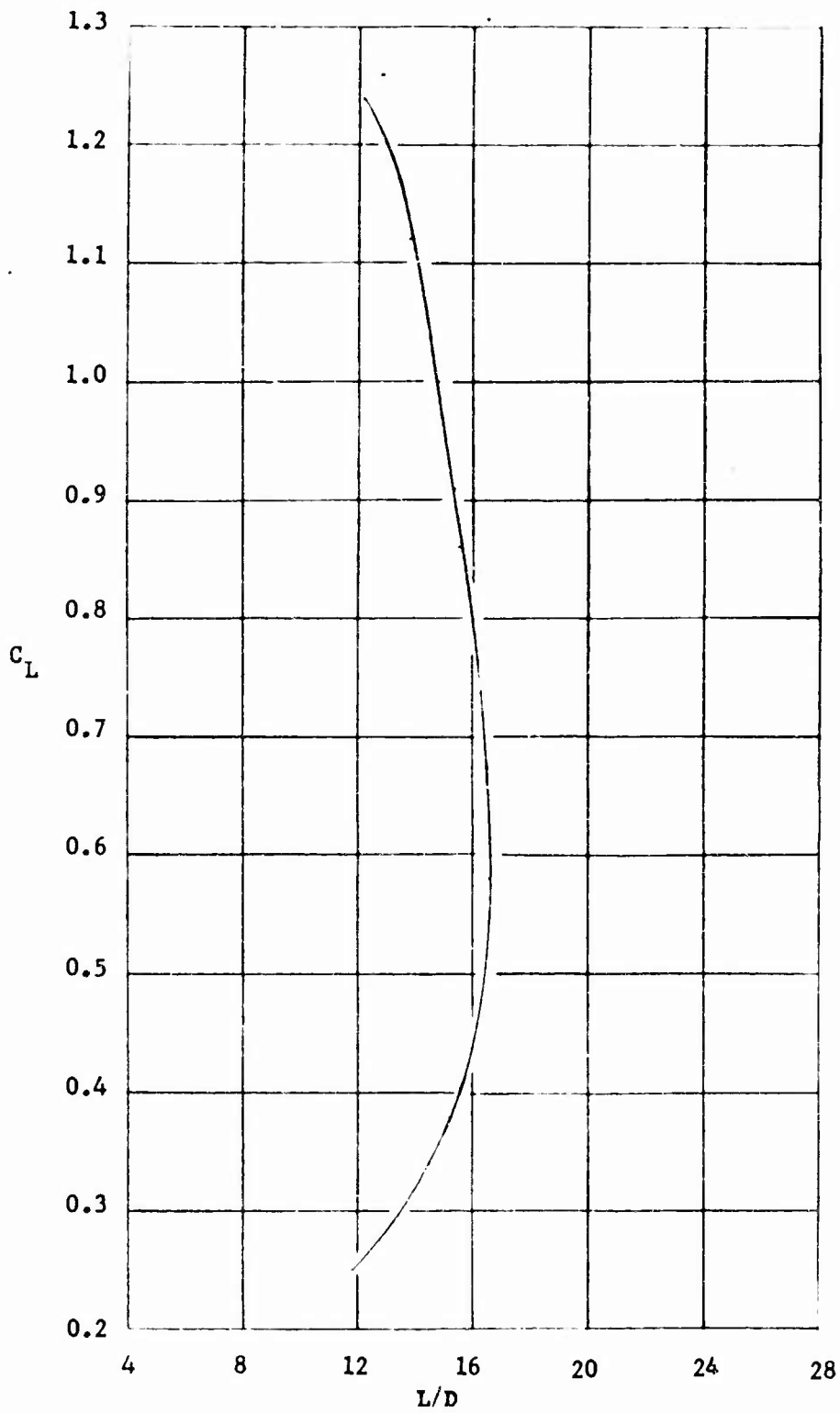


Figure 12 (Concluded)

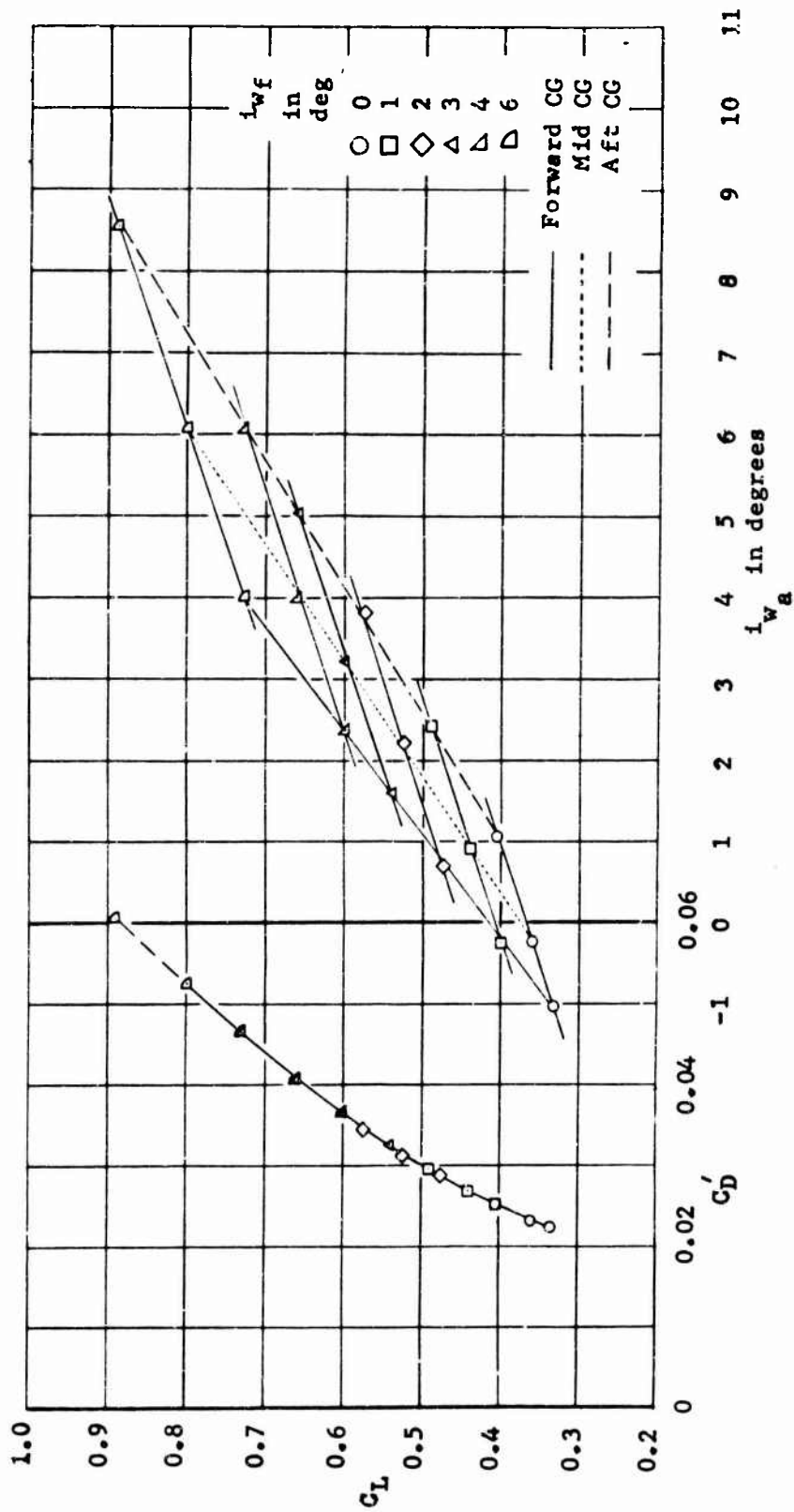


Figure 13 - Required  $i_{wa}$  for Trim of the TWIG Model Out of Ground Effect

(a)  $\alpha = 0^\circ$

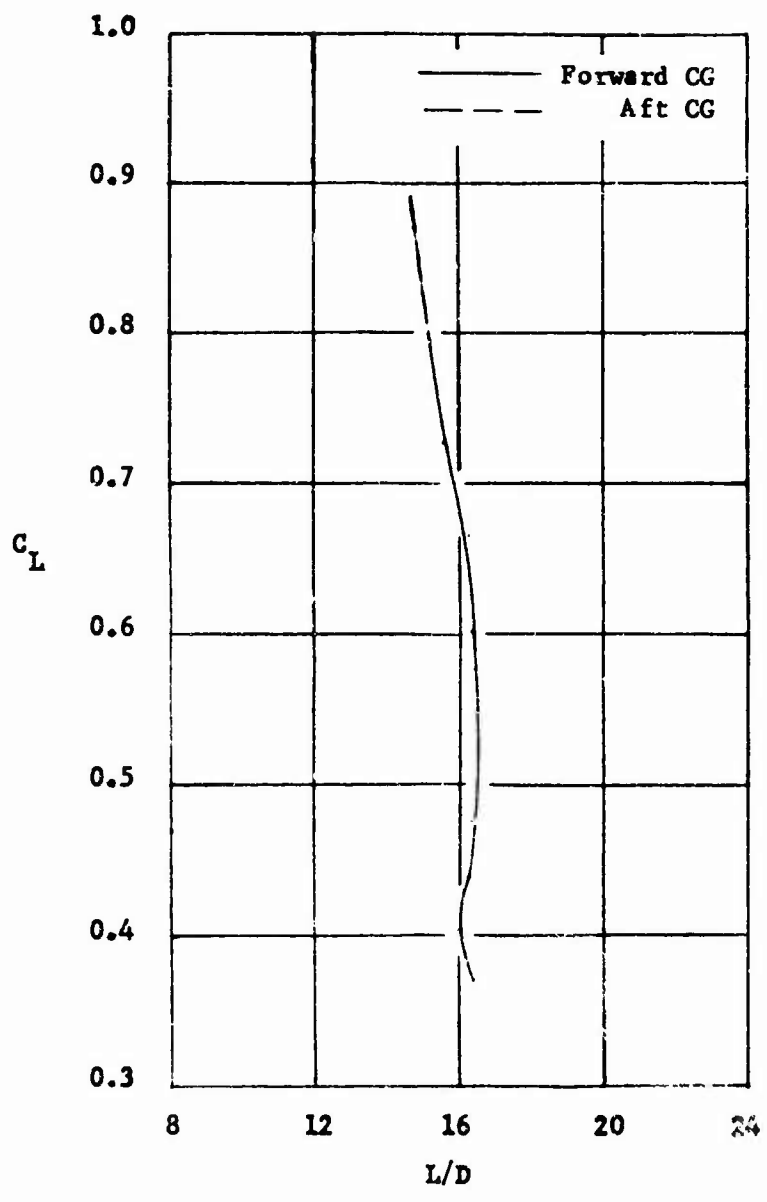


Figure 13 (Continued)  
 (a) Concluded

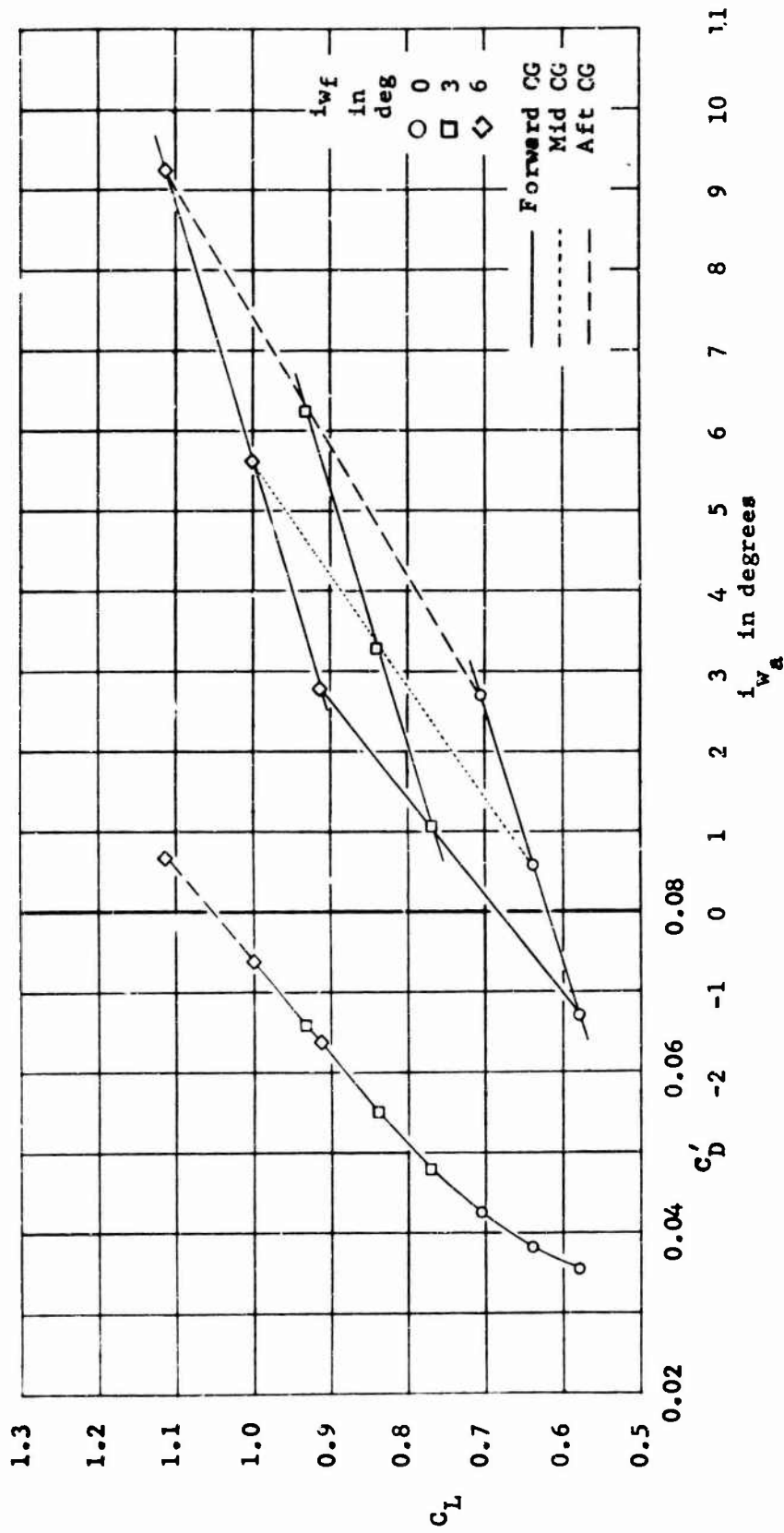


Figure 13 (Continued)  
(b)  $\alpha = 3^\circ$

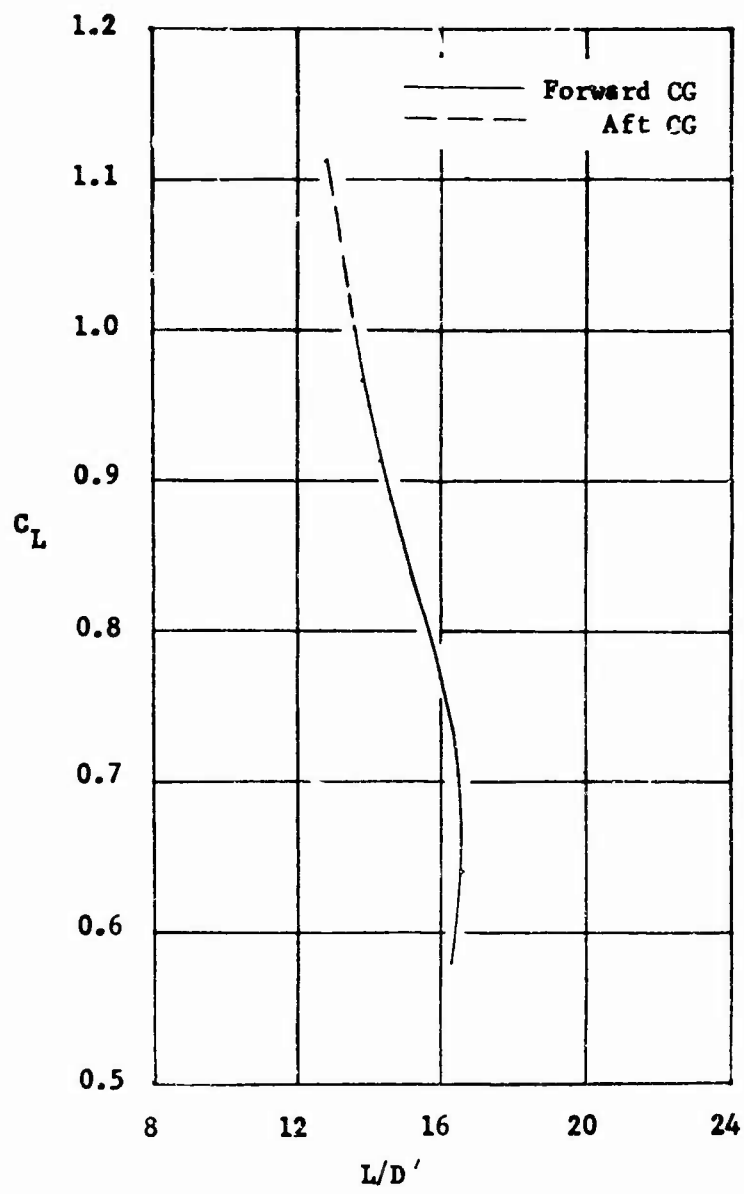


Figure 13 (Continued)  
 (b) Concluded

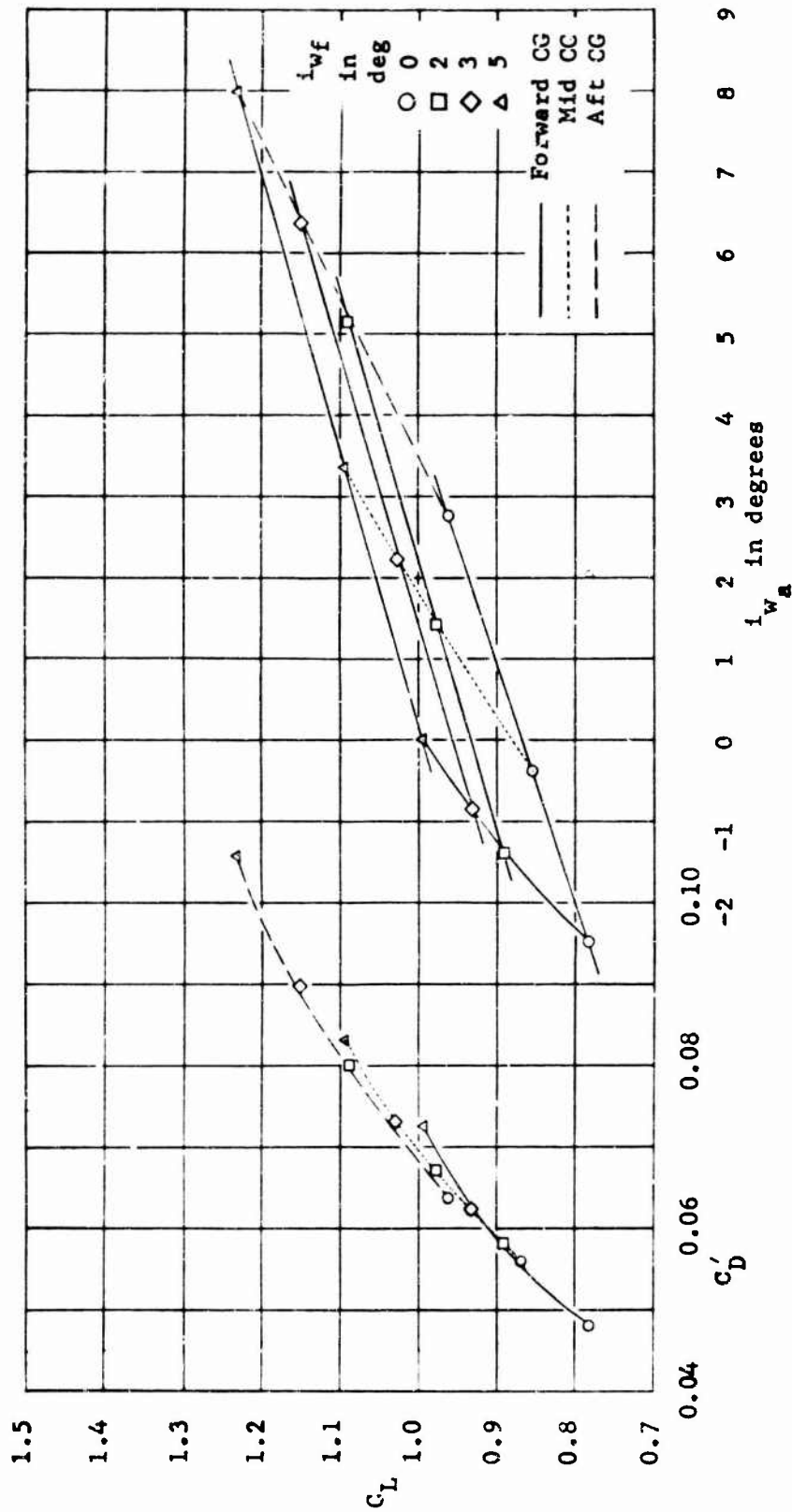


Figure 13 (Continued)  
(c)  $\alpha = 6^\circ$

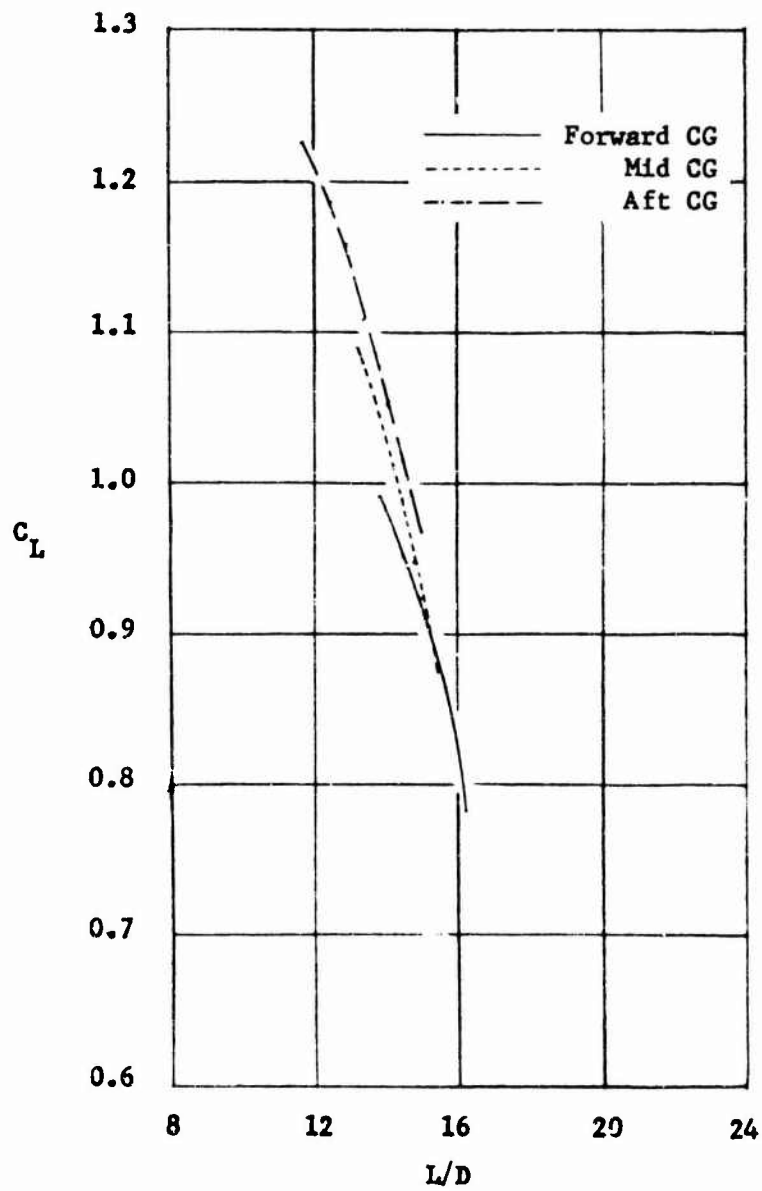


Figure 13 (Concluded)

(c) Concluded



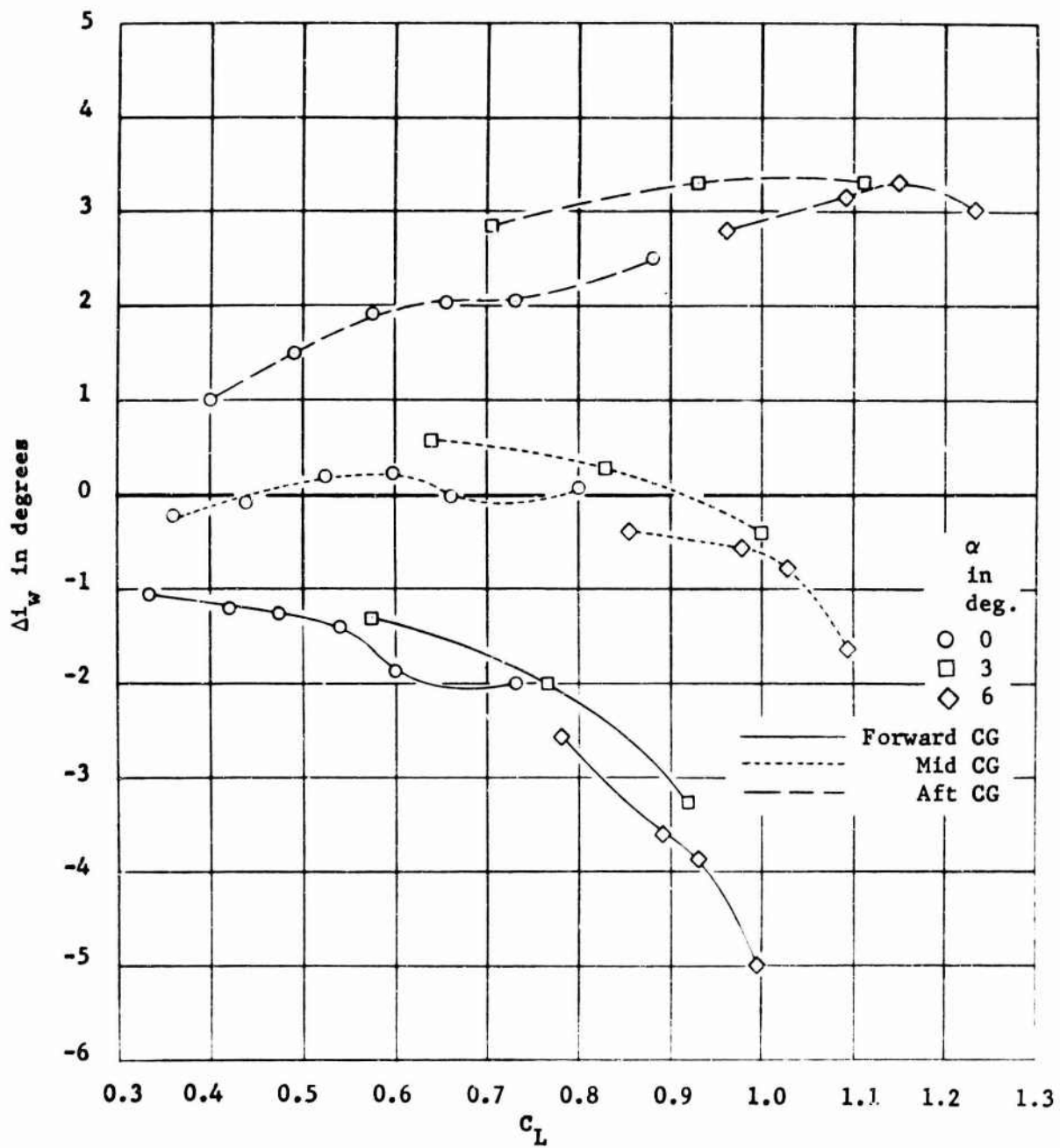


Figure 14 - Difference in Wing Incidence Angles Required for Trim of the TWIG Model Out of Ground Effect

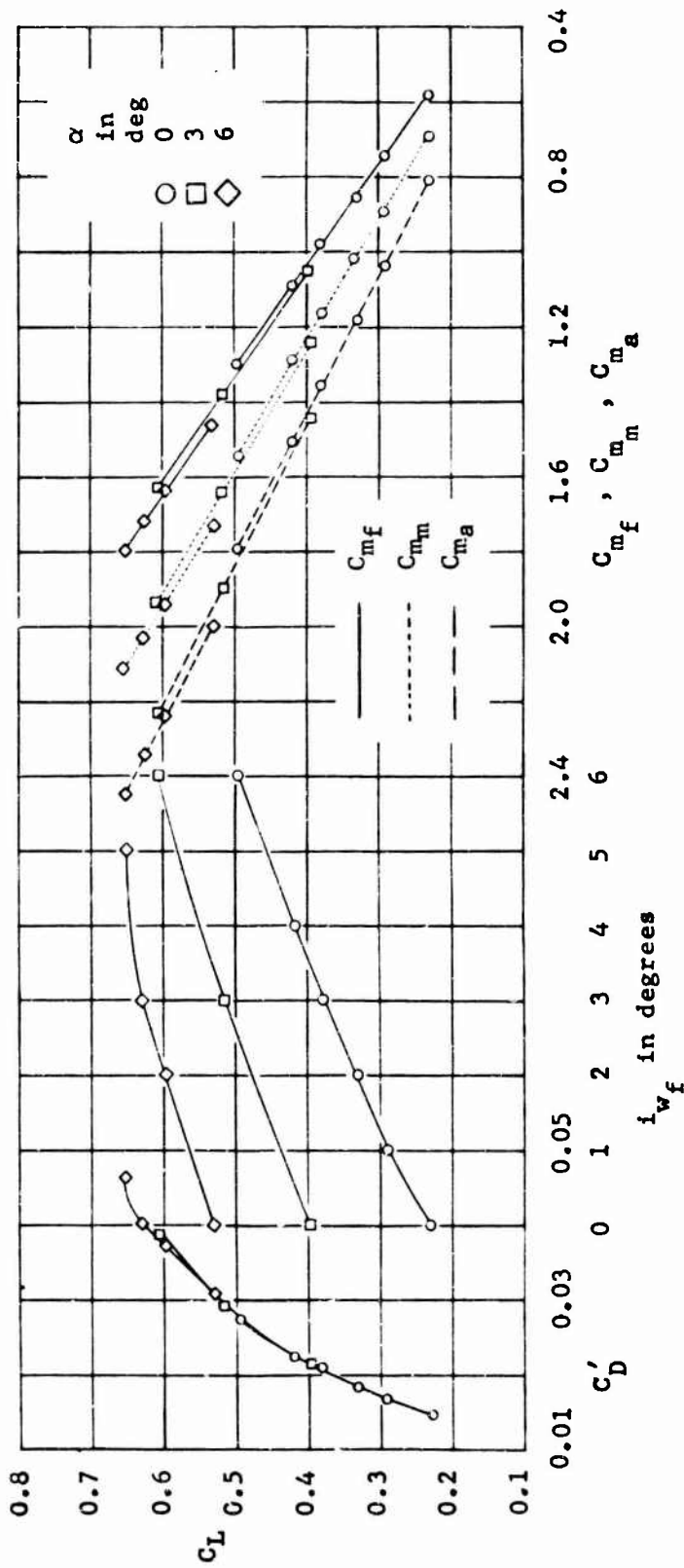


Figure 15 - Longitudinal Aerodynamic Characteristics of the TWIC Model  
Out of Ground Effect With the Aft Wing Removed

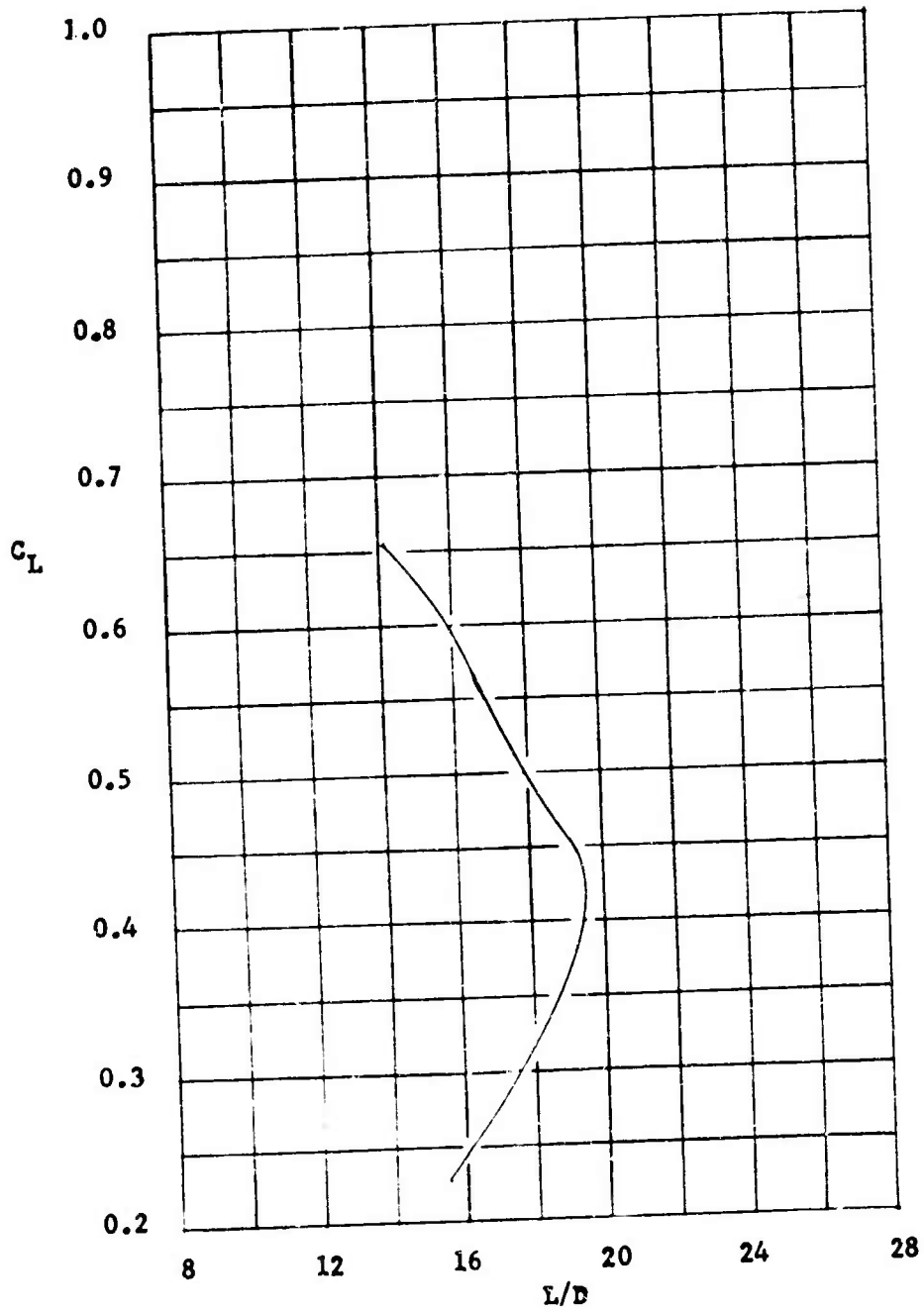


Figure 15 (Concluded)

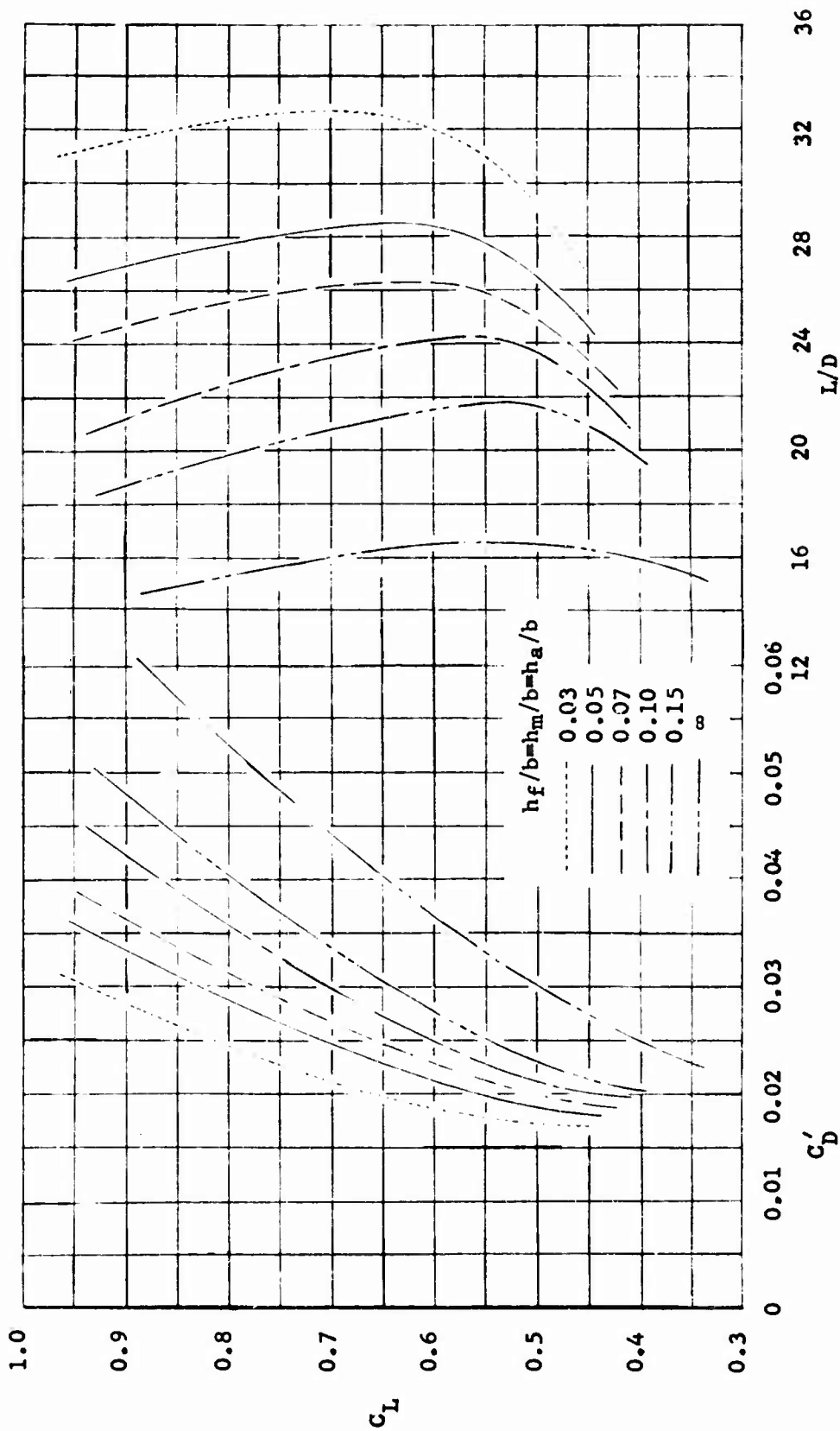


Figure 16 - Summary of TWIG Model Trim Data In and Out

of Ground Effect.  $\alpha = 0^\circ$

**BLANK**

Unclassified

Security Classification

DOCUMENT CONTROL DATA - R&D		
<i>(Security classification of title, body of abstract and indexing annotation must be entered when the overall report is classified)</i>		
1 ORIGINATING ACTIVITY (Corporate author) Aerodynamics Laboratory David Taylor Model Basin Washington, D. C. 20007		2a REPORT SECURITY CLASSIFICATION Unclassified
		2b GROUP
3 REPORT TITLE WIND TUNNEL INVESTIGATION OF AN ASPECT RATIO 10 TANDEM WING AIRCRAFT CONFIGURATION IN GROUND EFFECT PART I - LONGITUDINAL CHARACTERISTICS		
4 DESCRIPTIVE NOTES (Type of report and inclusive dates)		
5 AUTHOR(S) (Last name, first name, initial)  Harry, Charles W. and Trobaugh, Lynn A.		
6 REPORT DATE July 1966	7a TOTAL NO OF PAGES 71	7b NO OF REFS 4
8a CONTRACT OR GRANT NO. WEPTASK RAD348-001/440-1/P012-01-06	9a ORIGINATOR'S REPORT NUMBER(S)  Report 2259-1	
b PROJECT NO. Problem Assignment 1-34-52		
c d TMB 632-502	9b OTHER REPORT NO(S) (Any other numbers that may be assigned to this report)  Aero Report 1111-1	
10 AVAILABILITY/LIMITATION NOTICES  The distribution of this document is unlimited.		
11 SUPPLEMENTARY NOTES	12 SPONSORING MILITARY ACTIVITY Bureau of Naval Weapons Department of the Navy Washington, D. C. 20360	
13 ABSTRACT  Subsonic Wind-tunnel test results of a tandem wing aircraft configuration are given. Conventional longitudinal tests out of ground effect, and similar tests in ground effect, employing the ground board test technique, were conducted on the configuration. Test variables included height above the surface, forward and aft wing incidence angles, angle of attack, and center-of-gravity location.		

DD FORM 1473  
1 JAN 64

Unclassified

Security Classification

Unclassified  
Security Classification

14 KEY WORDS	LINK A		LINK B		LINK C	
	ROLE	WT	ROLE	WT	ROLE	WT
<p>Ground Effect</p> <p>Subsonic Wind Tunnel Tests</p> <p>Tandem Wings</p> <p>Wing Incidence</p> <p>Longitudinal Stability</p> <p>Aspect Ratio</p>						

**INSTRUCTIONS**

1. **ORIGINATING ACTIVITY:** Enter the name and address of the contractor, subcontractor, grantee, Department of Defense activity or other organization (*corporate author*) issuing the report.

2a. **REPORT SECURITY CLASSIFICATION:** Enter the overall security classification of the report. Indicate whether "Restricted Data" is included. Marking is to be in accordance with appropriate security regulations.

2b. **GROUP:** Automatic downgrading is specified in DoD Directive 5200.10 and Armed Forces Industrial Manual. Enter the group number. Also, when applicable, show that optional markings have been used for Group 3 and Group 4 as authorized.

3. **REPORT TITLE:** Enter the complete report title in all capital letters. Titles in all cases should be unclassified. If a meaningful title cannot be selected without classification, show title classification in all capitals in parenthesis immediately following the title.

4. **DESCRIPTIVE NOTES:** If appropriate, enter the type of report, e.g., interim, progress, summary, annual, or final. Give the inclusive dates when a specific reporting period is covered.

5. **AUTHOR(S):** Enter the name(s) of author(s) as shown on or in the report. Enter last name, first name, middle initial. If military, show rank and branch of service. The name of the principal author is an absolute minimum requirement.

6. **REPORT DATE:** Enter the date of the report as day, month, year, or month, year. If more than one date appears on the report, use date of publication.

7a. **TOTAL NUMBER OF PAGES:** The total page count should follow normal pagination procedures, i.e., enter the number of pages containing information.

7b. **NUMBER OF REFERENCES:** Enter the total number of references cited in the report.

8a. **CONTRACT OR GRANT NUMBER:** If appropriate, enter the applicable number of the contract or grant under which the report was written.

8b, 8c, & 8d. **PROJECT NUMBER:** Enter the appropriate military department identification, such as project number, subproject number, system numbers, task number, etc.

9a. **ORIGINATOR'S REPORT NUMBER(S):** Enter the official report number by which the document will be identified and controlled by the originating activity. This number must be unique to this report.

9b. **OTHER REPORT NUMBER(S):** If the report has been assigned any other report numbers (*either by the originator or by the sponsor*), also enter this number(s).

10. **AVAILABILITY/LIMITATION NOTICES:** Enter any limitations on further dissemination of the report, other than those

imposed by security classification, using standard statements such as:

- (1) "Qualified requesters may obtain copies of this report from DDC."
- (2) "Foreign announcement and dissemination of this report by DDC is not authorized."
- (3) "U. S. Government agencies may obtain copies of this report directly from DDC. Other qualified DDC users shall request through \_\_\_\_\_."
- (4) "U. S. military agencies may obtain copies of this report directly from DDC. Other qualified users shall request through \_\_\_\_\_."
- (5) "All distribution of this report is controlled. Qualified DDC users shall request through \_\_\_\_\_."

If the report has been furnished to the Office of Technical Services, Department of Commerce, for sale to the public, indicate this fact and enter the price, if known.

11. **SUPPLEMENTARY NOTES:** Use for additional explanatory notes.

12. **SPONSORING MILITARY ACTIVITY:** Enter the name of the departmental project office or laboratory sponsoring (*paying for*) the research and development. Include address.

11. **ABSTRACT:** Enter an abstract giving a brief and factual summary of the document indicative of the report, even though it may also appear elsewhere in the body of the technical report. If additional space is required, a continuation sheet shall be attached.

It is highly desirable that the abstract of classified reports be unclassified. Each paragraph of the abstract shall end with an indication of the military security classification of the information in the paragraph, represented as (TS), (S), (C), or (U).

There is no limitation on the length of the abstract. However, the suggested length is from 150 to 225 words.

14. **KEY WORDS:** Key words are technically meaningful terms or short phrases that characterize a report and may be used as index entries for cataloging the report. Key words must be selected so that no security classification is required. Identifiers, such as equipment model designation, trade name, military project code name, geographic location, may be used as key words but will be followed by an indication of technical context. The assignment of links, roles, and weights is optional.